Niche differentiation in both microhabitat and trophic interactions contributes to high local diversity of Euphorbiaceae in a tropical tree assemblage

Xue-Zhao Wang[1, 2 †], Shan-Wen Sun[3 †], Brian E. Sedio[4, 5], Suphanee Glomglieng[1, 2], Min Cao[1], Kun-Fang Cao[6], Jian-Hong Yang[7], Jiao-Lin Zhang[1]*, Jie Yang[1]*

[1] *CAS Key Laboratory of Tropical Forest Ecology, Xishuangbanna Tropical Botanical Garden, Chinese Academy of Sciences, Kunming 650223, China*

[2] *University of Chinese Academy of Sciences, Beijing 100049, China*

[3] *College of Life Sciences, Northeast Forestry University, Harbin 150040, China*

[4] *Department of Integrative Biology, University of Texas at Austin, Austin, TX, United States*

[5] *Smithsonian Tropical Research Institute, Apartado 0843-03092, Balboa, Ancón, Republic of Panama*

[6] *Plant Ecophysiology and Evolution Group, State Key Laboratory for Conservation and Utilization of Subtropical Agro-bioresources, Guangxi University, Nanning, Guangxi 530004, China*

[7] *State Key Laboratory of Phytochemistry and Plant Resources in West China, Kunming Institute of Botany, Chinese Academy of Sciences, Kunming 650201, China*

† These authors contributed equally to this work.

* Corresponding author: Jie Yang, E-mail: yangjie@xtbg.org.cn; Jiao-Lin Zhang, E-mail: zjl@xtbg.org.cn

Statement of authorship: J.Y., X.Z.W designed the study; X.Z.W performed the analysis; S.W.S., X.Z.W, S.G., K.F.C, J.Y., and J.L.Z collected and measured the data; X.Z.W., J.Y and B.E.S. wrote the manuscript, and all authors provided comments

Length: 4979 words in main text; 366 words in figure and table captions; 4 figures; 1 table; 92 references; 2 appendixes.

ABSTRACT

Understanding the mechanisms that drive community assembly in species-rich tropical forest remains a fundamental challenge in ecology. Here, we integrated trait dimensions, metabolomics, and phylogeny to test whether interspecific variation over multivariate trait dimensions contribute to coexistence among Euphorbiaceae species. We measured 41 functional traits related to resource acquisition, photosynthetic capacity, hydraulic safety and efficiency, and defense in all 26 Euphorbiaceae species in a 20-ha forest dynamics plot in tropical southwestern Yunnan, China. Network analysis revealed that a small number of traits with high network centrality reflected variation in ecological strategy among the Euphorbiaceae. Further, we observed significant turnover with respect to these high-centrality traits over environmental gradients at distinct spatial and temporal scales. Whereas resource-utilization traits and the habitat associations they mediate exhibited consistent phylogenetic signal. Phylogenetic divergence in chemical defenses likely represents an additional trait dimension that enhances local diversity of closely related Euphorbiaceae in southwestern China.

KEYWORDS: closely related species, convergent evolution, divergent evolution, Euphorbiaceae, herbivores, secondary metabolites, trait dimensions.

INTRODUCTION

Co-occurrence of numerous closely related species at a local scale is a hallmark of diverse tropical forests (Gentry, 1989). Understanding the mechanisms that maintain such diversity in the face of intense competition for resources remains a long-standing challenge in ecology. Closely related species are often phenotypically and ecologically similar due to phylogenetic conservatism and are likely to occupy similar niches (Harvey & Pagel, 1991; Wiens et al., 2010). Classical niche theory maintains that ecologically similar species should not stably coexist due to habitat overlap, resource competition, and shared natural enemies (Gause, 1934; Holt, 1977; Chesson, 2000). The idea that natural enemies with highly specialized host ranges may maintain plant diversity through conspecific negative density dependence (Janzen, 1970; Connell, 1971) has been proposed to an attractive potential solution to the paradox. Yet many insect herbivores and microbial pathogens are not single-host specialists (Novotny et al., 2002; Ødegaard & Diserud, 2005; Gilbert & Webb, 2007) and hence are likely to mediate competitive exclusion among plants within their host ranges (Chesson & Kuang, 2008; Sedio & Ostling, 2013). Fortunately, while plant lineages with high local species richness challenge our understanding of coexistence, the very tendency toward phylogenetic niche conservatism that makes the high local diversity of these lineages such an apparent paradox also makes them excellent study systems in which to tease apart the niche axes that underpin their diversity.

Identifying the niche differences that distinguish co-occurring, closely related plants require to measure traits and their interactions with the abiotic and biotic environment that they mediate. Recent research on 'functional' traits of plants suggests that variation in life-history strategy and environmental distribution may be highly multivariate in the space of measurable

morphological and physiological traits (Condit et al., 2013; Trisos et al., 2014; Laughlin & Messier, 2015; Rüger et al., 2018), even among closely related species (Sedio et al., 2012). Focus on a single dimension may overlook niche differentiation in other dimensions of trait or niche space and limit explanatory power, yet the integrated study of multivariate trait space and the interaction of multivariate dimensions with multiple axes of variation in the abiotic and biotic environment has the potential to reveal niche segregation that would not be reflected in a single dimension (Futuyma & Moreno, 1988; Yang et al., 2018; Burton et al., 2020).

In addition to morphological variation, much of the functional trait variation of plants is a result of small organic molecules that comprise the metabolome. The plan metabolome includes primary metabolites involved in core metabolic pathways and the molecular building blocks of large organic polymers, such as nucleotides, amino acids, and mono- and disaccharides. However, much of the interspecific variation in plants is a result of the astonishing diversity of secondary metabolites with specialized functions (Sedio et al., 2021; Walker et al., 2022). Secondary metabolites can mediate plant responses to abiotic stressors, such as ultraviolet radiation and freezing temperatures (Rasmann et al., 2014), and can serve as antinutritive agents or acute toxins against herbivores and pathogens (Coley, 1983) and play an important role in shaping natural enemy host ranges (Pagare et al., 2015; Salazar et al., 2018). Much like the shared resources, shared natural enemies such as insect herbivores and pathogens can mediate competitive exclusion of host plants (Chesson & Kuang, 2008; Sedio et al., 2013). But unlike abiotic stressors, natural enemies are capable of reciprocal coevolution in response to the evolution of chemical defenses on the part of their plant hosts, which may make them strong agents of selection for divergence in chemical composition and the evolution of novel

chemical defenses (Ehrlich & Raven, 1964; Schemske et al., 2009; Volf et al., 2020). The vast

diversity of plant secondary metabolites has long precluded the study of metabolomics at the

community scale. However, the recent rapid rise of ecological metabolomics (Sedio et al., 2018,

2021; Walker et al., 2022) promises to illuminate the role of plant secondary metabolites even

in species-rich and understudied communities such as tropical forests.

Closely related species are derived from a recent common ancestor and hence expected to

exploit a limited range of trait space. Furthermore, closely related species are expected to be

more ecologically similar than distantly related species (Ackerly, 2004; Burns & Strauss, 2011).

For these reasons, divergence along trait or niche axes among closely related species should be

observable against a phylogenetically conserved background and help to reveal the niche

dimensions along which interspecific differentiation has contributed to the diversification of,

and maintenance of diversity within, the lineage (Ackerly, 2004; Ackerly et al., 2006; Swenson,

2011; Sedio et al., 2012; McKown et al., 2016). Traits are likely to evolve as correlated suites

or syndromes that reflect ecological tradeoffs in function (Wright et al., 2004; Kursar & Coley,

2003). Hence, consideration of phylogenetic patterns with respect to multivariate trait space

may reveal conservation or divergence in multivariate ecological strategies (Rüger et al., 2020).

Finally, a comparison of phylogenetic patterns among multiple axes of trait variation can reveal

which niche dimensions have played a role in ecological differentiation within a plant lineage

and at what phylogenetic scale, for example at the crown or at the tips of the phylogeny. For

example, Sedio et al. (2012) found that hydraulic traits were phylogenetically conserved among

the *Psychotria* of Barro Colorado Island, Panama, resulting in fine-scale co-occurrence of close

relatives in shared hydraulic niches, whereas photosynthetic traits were more variable.

6

Similarly, Vleminckx et al. (2018) observed phylogenetically conserved resource-use strategies, but phylogenetic divergence in defenses. There is growing evidence of widespread phylogenetic divergence in secondary metabolites within tropical tree lineages (Becerra, 1997; Kursar et al., 2009; Sedio, 2017). However, few studies have integrated the comprehensive study of morphological and physiological traits related to resource-utilization strategy with a metabolomics-based study of variation in secondary metabolites in a community and phylogenetic context.

Here, we assessed interspecific, ecological, spatial, and phylogenetic variation in morphological, physiological, and chemical traits to identify the key axes of variation that contribute to the high local diversity of trees in a single plant family in a local community. We measured 41 functional traits related to resource acquisition, photosynthetic capacity, hydraulic conductivity and efficiency, and defense in all 26 free-standing woody species of Euphorbiaceae in tropical seasonal rain forest in Xishuangbanna, southwestern China. We examined the correlation structure of interspecific variation among these 41 traits using a trait networking approach (Messier et al., 2017) and detected the interspecific variation in leaf secondary metabolites through the use of untargeted metabolomics (Sedio et al., 2018, 2021). We coupled these traits with detailed measurements of variation in soil nutrients, light environment, soil water content and herbivore pressure within the plot to identify the axes of trait variation that may define niche differences among co-occurring woody Euphorbiaceae with the potential to facilitate ecological coexistence through segregation along key abiotic and biotic gradients. Specifically, we asked: (i) Do a few traits with central correlational relationships can reflect interspecific variation in ecological strategy among co-occurring

Euphorbiaceae? (ii) Do interspecific variation along multivariate trait dimensions contribute to niche partitioning among locally co-occurring species by segregating Euphorbiaceae over abiotic and biotic gradients in time and space? and (iii) Do major axes of trait variation differ in phylogenetic signal, and hence the phylogenetic scale at which they contribute to niche differentiation among the Euphorbiaceae in a tropical tree community?

MATERIALS AND METHODS

Study site

The study was conducted in a seasonal tropical rainforest dynamics plot (FDP) in Xishuangbanna, southwestern China (101°34E, 21°36′N; FIGURE 1A). The most dominant family in the plot is Icacinaceae, followed by Lauraceae and Euphorbiaceae, based on the importance index (Lan et al., 2008). The mean annual temperature is 21.8 °C and the mean annual precipitation is 1492.9 mm in the plot. The forest is influenced by a tropical monsoonal climate, with 84% of mean annual precipitation (1246 mm) occurring during the rainy season from May to October, and a long dry season that lasts from November to next April. Soil type in the plot is mainly laterite with deep soil layers and thin humus (Cao et al., 2006). Habitat heterogeneity was caused by the three perennial streams which traverse the plot and merge together at the southeastern corner. The 2012 census recorded a total of 392 tree species belonging to 196 genera and 69 families represented by individuals with ≥ 1 cm diameter at breast height.

Focal species

All 26 species of Euphorbiaceae (Appendix S2: TABLE S1) in the plot were selected as focal species for the following reasons: (1) Euphorbiaceae is one of the largest families of all flowering plants (Ernst et al., 2015) and nearly global in distribution with the exception of boreal areas, although it is more abundant in tropical regions (Rahman & Akter, 2013). (2) Euphorbiaceae ranked third with respect to the importance value among families in our plot, including 9,827 individuals with DBH > 1 cm and 25.51% of the total basal area (Lan et al., 2008, FIGURE 1B). (3) Euphorbiaceae includes both pioneer and late successional species, components of both the canopy layer and understory, and is distributed from valley to ridge, reflecting variations in resource acquisition ability, photosynthesis capacity, shade tolerance and water requirements (Davies et al., 1998). (4) Most species of the Euphorbiaceae have extraordinary chemical diversity and these chemical compounds are thought to play an important ecological role through herbivore feeding deterrence and antimicrobial activity (Vasas & Hohmann, 2014). Thus, Euphorbiaceae provides an excellent system to examine niche segregation and assembly among closely related species.

Functional traits measurements

To explore the species coexistence with respect to multiple niche axes, we classified functional traits into five multivariate dimensions based on specific ecological functions (Appendix S2: TABLE S2). We collected 13 traits for resource acquisition, 8 traits for photosynthetic ability, 11 hydraulic traits, 8 physical defensive traits and secondary metabolites representing variation in chemical defense (FIGURE 1C; Appendix S2: TABLE S3). See

9

Appendix S1 for detailed functional trait measurements. Descriptive statistics of 40 functional traits are reported in **Appendix S2: TABLE S4.**

Environmental variables

Numerous environmental parameters have been proposed to be major drivers of species distributions. We measured soil nutrient properties, soil water content, light environment and insect herbivory to provide environmental context for species variation in traits that mediate resource acquisition, hydraulic ability, photosynthetic capacity and defensive ability (Sun et al., 2016; Both et al., 2019; Rosas et al., 2019). Soil available nitrogen (N), extractable phosphorus (P), extractable potassium (K), total carbon (C) and soil water content was published in Yang et al., 2014. Light environment was measured using a digital camera with a fisheye lens (Nikon FC-E8 Fisheye Converter, Nikon Corporation, Japan) to take hemispherical photographs in low light conditions in each quadrat. We used the software Gap Light Analyzer Version 2.0 to analyze all images, in which light environment was quantified as the fraction of the image not occupied by vegetation cover (Frazer et al., 2000).

To quantify herbivore pressure, we measured herbivory on all species of Euphorbiaceae encountered (Halpern et al., 2010). We randomly selected five mature individuals with height ranging from 5 to 6 meters for each species (Caldwell et al., 2016), and for each individual, three branches were taken from each direction and 10 leaves per branch were selected beginning from the tip. All collected leaves were scanned (Epson Co., Beijing, China), and leaf area was calculated using ImageJ (Abramoff et al., 2004). We measured the percent loss in area for each leaf by comparing the damaged leaf area to the area of the inferred intact leaf shape

using the scanned images (Kurokawa & Nakashizuka, 2008). For each leaf, we calculated the herbivory ratio as the ratio of the damaged area to the estimated undamaged area of the leaf (i.e., leaves that suffered greater herbivore damage have a higher herbivory ratio). We classified herbivore damage as hole feeding and marginal feeding based on the guide of distinctive patterns of damage (Labandeira et al., 2007). According to leaf damage types, we also divided these insect herbivory types into three diet breadth categories: generalized, intermediate or specialized.

Principal component analysis (PCA) was conducted on each type of environmental factor to reduce the trait data into major orthogonal axes. We utilized the first three principal components for further analysis of environment distance (Appendix S2: TABLE S5, S6).

Network analysis: Exploring trait and trait-dimension correlations

We evaluated relationships between measured traits and broad, multi-trait dimensions using network analysis in which we calculated the connectivity and distance properties of interconnected traits. We used Pearson's correlation to calculate the observed trait correlations. Pairwise trait correlations with $r > 0.2$ were significant at $p < 0.05$ and were shown in the network. We calculated the indicator of "degree" following Messier et al. (2017), which is the number of connections leading to a trait. Through this network analysis, we screened traits with large degree values one by one and selected the top four traits with large degree values in each trait dimension. In subsequent analyses, we explored the environmental and spatial turnover with respect to these top four traits with the greatest 'centrality' in each dimension (centrality) and with respect to all traits in each trait dimension (all).

11

To explore the degree of trait integration that characterizes interspecific variation with respect to major dimensions representing resource-acquisition photosynthetic, hydraulic, and physical-defense traits among the Euphorbiaceae, we employed a network-based hypothesis-testing framework following Messier et al. (2017). For each of the four major trait dimensions, we compared two alternative hypotheses: the hypothesis that four traits with high network centrality describe interspecific variation ($H_{CENRALITY}$) and the hypothesis that interspecific variation is better described using all measured traits (H_{ALL}). For each hypothesis test, we used standardized *Mantel's* tests, which calculate the Pearson's correlation coefficient for two correlation matrices (Zuur et al., 2007): the hypothesized correlation matrix ($H_{CENTRALITY}$ or H_{ALL}) and the observed trait correlation matrix (D) calculated from our empirical data (Cheverud et al., 1989). We repeated these hypothesis tests for $H_{CENTRALITY}$ and H_{ALL} for each of four major trait dimensions (Appendix S2: TABLE S8-S11). We did not have specific hypotheses regarding the relative strengths of trait correlations, so we only included values of -1, 0 and 1 in the hypothesis matrices. For all traits, if the relationship between traits was expected to be positive, it was set to 1, if it was expected to be negatively correlated, it was set to -1, and if no relationship between traits was expected, it was set to 0, with expectations based on Messier et al. (2017). For $H_{CENTRALITY}$, the correlation value was set to 0 if one of the traits was not a high-centrality trait and -1 or 1 for pairs of high-centrality traits (Yang et al., 2019; Yao et al., 2021). Note that these values do not test whether the correlations are perfect, but simply specify the signs of the correlation.

Functional-trait turnover along environmental gradients

To test functional-trait turnover along environmental dimensions, we first calculated functional beta diversity between subplots at local scale on 20 m × 20 m. For each of the five trait dimensions, we calculated the functional dissimilarity between each pair of subplots using the trait distance (D_{pw}) of the four traits with the greatest centrality values and all functional traits (Ricotta & Burrascano, 2008). D_{pw} was calculated as follows:

$$D_{pw} = \frac{\sum_{i=1}^{n_{k1}} \overline{\delta}_{ik2} + \sum_{j=1}^{n_{k2}} \overline{\delta}_{jk1}}{n_{k1} + n_{k2}}$$

where n_{k1} represents the number of species in community $k1$; n_{k2} represents the number of species in community $k2$; $\overline{\delta}_{ik2}$ is the mean pairwise trait distance between species i in community $k1$ to all species in community $k2$ and $\overline{\delta}_{jk1}$ is the mean pairwise trait distance between j species in community $k2$ to all species in community $k1$; $min\,\delta_{ik2}$ is the nearest trait distance between species i in community $k1$ to all species in community $k2$ and $min\,\delta_{jk1}$ is the nearest trait distance between species j in community $k2$ to all species in community $k1$.

We used generalized additive models (GAMs; Wood, 2006) to test for significant nonlinear pattern of our hypothesized relationships between environmental drivers and turnover in functional traits in each dimension. For the GAMs, we restricted the number of knots to three in order to avoid locally overfitting the data but still allowing unimodal or slightly more complex model fits. In order to identify the most relevant and best fitting environmental driver for each functional trait dimensions, we calculated GAMs for the turnover of each

functional trait with environmental distance. We also estimated functional-trait turnover with respect to spatial distance.

Phylogenetic signal of traits and trait dimensions

A phylogenetic tree of Euphorbiaceae was reconstructed based on previously reported DNA barcode sequences (Yang et al., 2014). A DNA supermatrix was generated from three chloroplast regions – *r*bcL, *matK*, *trnH-psbA* – and the nuclear ribosomal internal transcribed spacer (ITS). See Yang et al. (2014) for detailed methods of phylogenetic tree reconstruction. To evaluate whether functional traits and trait dimensions exhibit different phylogenetic models, we calculated Blomberg's *K* statistic for the four traits with the greatest centrality values in each dimension and for all functional traits except secondary metabolites (Blomberg et al., 2003). We tested whether *K* was significant by randomizing the trait values 999 times across the phylogeny and calculating the number of times the randomized trait data resulted in a higher value of *K* than the observed value (Münkemüller et al., 2012). This number was then divided by the total number of randomizations to get a *P*-value, with $P \leq 0.05$ indicating significant phylogenetic signal.

To measure phylogenetic signal in a manner that could be directly compared between morphological and physiological traits and pairwise chemical similarity, we used a method based on phylogenetically independent contrasts (PICs) following Sedio et al. (2018). For each node in the phylogeny, we calculated the mean CSCS for species pairs for which the node was the most recent common ancestor (MRCA). We refer to this metric, which is defined for each node in the phylogeny, as $CSCS_{mrca}$. To evaluate phylogenetic signal, trait phylogenetic

disparity (or 1-CSCS_{mrca} in the case of secondary metabolites) was regressed against log-transformed phylogenetic distance, where $|t| \geq 1.96$ ($P \leq 0.05$) indicates significant phylogenetic signal. All analyses were performed using the R packages "*igraph*", "*geoR*", "*spdep*", "*ecodist*", "*vegan*" and "*picante*" (Ribeiro Jr & Diggle, 2001; Goslee & Urban, 2007; Bivand, 2010; Kembel et al., 2010; Oksanen et al., 2015).

RESULTS

The relationship between traits and trait dimensions

We conducted network analysis for all traits to test for trait relationships between and within dimensions representing resource acquisition, photosynthetic, hydraulic and physical defensive traits and to find traits with a high degree of centrality (Appendix S2: TABLE S7). Different traits were connected between and within trait dimensions except max tree height, showing that different trait dimensions do not form distinct modules (FIGURE 2). *Mantel's* test provided support for the hypothesis that four traits with large 'degree' values ($\textbf{\textit{H}}_{\textbf{CENTRALITY}}$) were significantly correlated with our empirical data (TABLE 1; $P \leq 0.05$) and further implied that interspecific variation with respect to these high-centrality traits represents species-level variation in all the traits in each dimension. For photosynthetic and physical-defense traits, four traits with large 'degree' values better reflected our empirical data than did all traits in each trait category, with $r_M = 0.64$ and $r_M = 0.34$ for photosynthetic and physical-defense traits, respectively. For resource acquisition and hydraulic traits, all traits ($\textbf{\textit{H}}_{\textbf{ALL}}$) better reflected our empirical data ($r_M = 0.44$ and 0.36, respectively) than did four traits with large 'degree' values in the trait network ($r_M = 0.29$ and 0.30, respectively).

Turnover in functional-trait dimensions along environmental gradients

We calculated the beta diversity of each trait dimension to explore how traits varied with environment and spatial distance at a local scale (FIGURE 3). Similarity with respect to trait dimensions that reflect photosynthetic traits, hydraulic traits, resource-acquisition traits and physical defenses significantly decreased with increasing environmental and spatial distance (FIGURE 3 A-D, $P < 0.001$), indicating that these functional traits turned over along environmental gradients and spatial distance to a greater extent than expected by chance. In contrast, similarity of secondary metabolites increased with average herbivory distance in the local scale and then stabilized (FIGURE 3 E, $P < 0.001$). In addition, the turnover with respect to axes representing functional traits was significantly greater with environmental distance than spatial distance, especially for physical defensive traits and secondary metabolites at large spatial scales.

Phylogenetic signal in functional trait dimensions

We measured the phylogenetic signal of all 41 functional traits and 16 traits with the greatest 'degree' values in each trait dimension to test whether functional traits and trait dimensions plus secondary metabolites varied in the phylogenetic signal within the community. Most resource-acquisition, photosynthetic and hydraulic traits and trait dimensions showed significant phylogenetic signal (FIGURE 4; Appendix S2: TABLE S12, 13; $P < 0.05$). Specifically, photosynthetic traits stomatal limitation (Ls) and canopy openness (CO) and hydraulic traits water use efficiency (WUE) and relative capacitance at turgor loss (C_{tlp})

16

exhibited strong phylogenetic signal (Blomberg's $K > 1$; Appendix S2: TABLE S12, 13). However, almost all physical-defense traits and secondary-metabolite similarity exhibited no significant phylogenetic signal (FIGURE 4; Appendix S2: TABLE S12, 13; $P > 0.05$).

DISCUSSION

The co-occurrence of numerous closely related species challenges expectations of species coexistence, but also presents an opportunity to better understand the mechanisms that generate and maintain diversity in tropical forests. Here, we have explored multiple dimensions of variation in morphological, physiological, and chemical functional traits to identify key axes that may contribute to niche segregation among co-occurring confamilial species. Our results revealed substantial differentiation in trait dimensions related to photosynthetic, hydraulic, resource-acquisition and defensive strategies with the potential to contribute to species coexistence by allowing species to segregate with respect to variation in resource availability and herbivore pressure over time and space. Yet, resource-acquisition traits exhibited phylogenetic signal, the diversity of closely-related Euphorbiaceae within the Xishuangbanna forest is likely further enhanced by phylogenetic divergence among the closest relatives with respect to secondary metabolites. We conclude that differentiation in chemical anti-herbivore defenses among closely related species may define another key trait axis that elevates species community richness beyond what would be supported by resource and habitat-defined niche partitioning alone.

Resource-utilization and defense traits exhibit contrasting community patterns

17

Interspecific competition for resources is expected to result in the competitive exclusion of inferior competitors from a community (Palmer, 1994). Competitive exclusion can be avoided, and species coexistence maintained, if species differ in their niche, such as their abiotic requirements and biotic interactions, such that intraspecific competition is stronger than interspecific competition and hence intraspecific negative feedback prevents complete exclusion of competitors (Chesson, 2000). Species differ in intrinsic fitness; the greater the differences in fitness, the greater niche differences must be to stabilize coexistence among competitors (Adler et al., 2007).

In a forest, the most obvious opportunities for niche segregation among tree species are habitats defined by spatial heterogeneity in edaphic resources, soil moisture, and light. Variation in species abundances over environmental gradients are mediated by morphological and physiological traits. Turnover with respect to traits can reflect filtering that habitat variation exerts on local assemblages, which provides a window on niche segregation among co-occurring species (Condit et al., 2000; Ravenscroft et al., 2014; Le Bagousse-Pinguet et al., 2017). A previous study demonstrated trait turnover with respect to both geographic and environmental distance within the Xishuangbanna plot (Yang et al., 2015). Here, we observed greater turnover in mean trait values of subplots with respect to environmental distance than simple geographic distance among subplots (FIGURE 3). Differences between mean photosynthetic, hydraulic, resource-acquisition, and physical-defense traits all increased with increasing distance in light, soil moisture, soil resources, and herbivory, respectively (FIGURE 3A-C). This turnover likely reflects species differences in abiotic niches that vary over fine-scale gradients in soil, moisture, and light.

Our results for the Euphorbiaceae at Xishuangbanna are largely concordant with other recent studies of trait turnover. For example, Fine et al. (2006) and Vleminckx et al. (2018) found significant turnover in functional traits related to resource acquisition in *Protium* with increasing dissimilarity of soil texture and nutrient availability, but little turnover with respect to secondary metabolites along these same environmental axes. Fortunel et al. (2014) demonstrated that functional turnover for 15 traits related to leaf and wood strategies and resource acquisition was strongly related to an edaphic gradient in lowland Amazonian forests in Peru and French Guiana. Our results further support the hypothesis that niche partitioning with respect to habitat heterogeneity contributes to the maintenance of species diversity in locally species-rich tree lineages at intermediate to large spatial scales.

In addition to abiotic resource requirements, trees exhibit a fundamental trade-off between growth rate and survival (Rüger et al., 2018, 2020), which manifests at the extremes as species that grow fast in high-resource (especially high-light) environments but invest comparatively little in defense and those that grow slowly in resource-poor environments but invest heavily in defense (Coley, 1983). We observed significant heterogeneity in herbivore pressure within the forest plot (FIGURE S1), likely driven by variation in light availability and hence productivity. Likewise, the turnover we observed in physical defenses was greater with respect to variation in herbivory than with spatial distance (FIGURE 3D), most likely because physical defenses were low and herbivory were high in high-resource environments, particularly canopy gaps (Coley, 1983).

Competition mediated by shared natural enemies is equivalent to resource competition in its capacity to mediate competitive exclusion (Chesson & Kuang, 2008), hence species

differences with respect to secondary metabolites that shape insect and pathogen host ranges can define niche differences that stabilize coexistence (Janzen, 1970; Connell, 1971; Sedio & Ostling, 2013). The turnover we observed in secondary metabolites with either spatial distance or distance defined in terms of similarity of herbivory rates was much less than that observed for other traits (FIGURE 3). This is likely because natural enemies that respond to the density of host plants promote local neighborhoods of chemically dissimilar individuals, which tends to reduce turnover in chemistry at larger spatial scales (Sedio & Ostling, 2013).

Resource-utilization and defense traits exhibit contrasting phylogenetic signal

Evaluating the phylogenetic signal in functional traits can provide an opportunity to assess the interaction between trait evolution and community assembly (Kembel & Hubbell, 2006). Our results indicate that most resource-acquisition, photosynthetic and hydraulic traits exhibit significant phylogenetic signal (FIGURE 4, Appendix S2: TABLE S12, 13). The phylogenetic signal in hydraulic traits that we observed among the Euphorbiaceae of Xishuangbanna is reminiscent of that observed among the *Psychotria* (Rubiaceae) of Barro Colorado Island, Panama (Sedio et al., 2012). More broadly, our results are consistent with a previous evaluation of phylogenetic signal in a wide range of functional traits in the Xishuangbanna plot as a whole (Yang et al., 2014) as well as studies in other tropical forest plots such as those at Yasuní, Ecuador (Kraft & Ackerly, 2010) and BCI, Panama (Westbrook et al., 2011). Our observations of trait turnover with environmental distance suggest that species of Euphorbiaceae exploit distinct habitats within the forest plot based on their morphological and physiological adaptations, and habitat filtering selects a subset of species with traits appropriate for the local

environment. The phylogenetic signal we observed for functional traits implies that these habitat differences facilitate niche segregation primarily among distantly related species, while potentially exacerbating competitive interactions among physiologically similar, closely related species of Euphorbiaceae.

In contrast to physiological traits related to resource acquisition, species similarity with respect to secondary metabolites did not exhibit phylogenetic signal (FIGURE 4, Appendix S2: TABLE S12, 13). This result is consistent with a growing number of studies of secondary metabolites in tropical tree lineages, including *Bursera* (Burseraceae) in Mexico (Becerra, 2007), *Eugenia* (Myrtaceae), *Inga* (Fabaceae), *Ocotea* (Lauraceae), *Piper* (Piperaceae), *Psychotria*, and *Protium* (Burseraceae) in Panama (Kursar et al., 2009; Sedio et al., 2018), *Ficus* (Moraceae) in Papua New Guinea (Volf et al., 2018), *Piper* in Costa Rica (Salazar et al., 2016), and *Inga* and *Protium* in Peru (Endara et al., 2017; Salazar et al. 2018; Vleminckx et al., 2018). Such commonplace divergence in secondary metabolites among closely related plants is likely driven by selection by insect herbivores and microbial pathogens that suppress local assemblages of chemically similar hosts (Sedio & Ostling, 2013; Forrister et al., 2019; Wink, 2018; Erb & Kliebenstein, 2020), thereby favoring the evolution of novel chemical defenses. Hence, our results contribute to an emerging consensus that species composition with respect to secondary metabolites may be more evolutionarily labile than morphological and physiological traits that mediate plant interactions with the abiotic environment. This has important implications for our understanding of the relative contribution of niche segregation with respect to traits that mediate plant interactions with the abiotic and biotic environment, as divergence in secondary metabolites that permits closely related species to avoid sharing

herbivores and pathogens may significantly enhance diversity beyond that maintained by segregation according to relatively phylogenetically conserved physiological niches.

CONCLUSION

Identifying the factors that permit closely related species to co-exist in species-rich tropical forests continues to be a major challenge in ecology. Traditional functional trait-based approaches explore this by a handful of traits data, but lack of solid evidence to explain this apparent paradox. Our results indicate that a small number of traits with high network centrality within the Euphorbiaceae reflect interspecific variation in ecological strategy with respect to global trait dimensions, representing resource acquisition, photosynthetic capacity, drought resistance and hydraulic efficiency, and physical defense. Furthermore, analyses of turnover with respect to environmental gradients suggest that species differences among multiple axes of trait variation may contribute to species coexistence in the Xishuangbanna forest by allowing Euphorbiaceae to exploit distinct microhabitats defined in terms of light, moisture, and soil nutrients. These physiological niche differences exhibit phylogenetic signal, whereas secondary metabolites do not, possibly as a result of diversifying selection by insect herbivores and pathogens. Our results suggest that phylogenetic divergence among closely related species with respect to secondary metabolites may enhance the local diversity of Euphorbiaceae beyond that supported by resource-based niche segregation by promoting coexistence among close relatives with similar habitat preferences in tropical rainforest.

AUTHOR CONTRIBUTIONS

J.Y., X.Z.W designed the study; X.Z.W performed the analysis; S.W.S., X.Z.W, S.G., K.F.C, J.Y., and J.L.Z collected and measured the data; X.Z.W., J.Y and B.E.S. wrote the manuscript, and all authors provided comments.

DATA ACCESSIBILITY

The data will be accessible in the Dryad Digital Repository if it is accepted.

REFERENCES

Abramoff, M., Magalhães, P. & Ram, S.J. (2004). Image processing with ImageJ. *Biophotonics International*, 11, 36-42.

Ackerly, D.D. (2004). Adaptation, niche conservatism, and convergence: comparative studies of leaf evolution in the California chaparral. *The American Naturalist*, 163, 654-671.

Ackerly, D.D., Schwilk, D.W. & Webb, C.O. (2006). Niche evolution and adaptive radiation: testing the order of trait divergence. *Ecology*, 87, S50-S61.

Adler, P.B., Hillerislambers, J. & Levine, J.M. (2007). A niche for neutrality. *Ecology Letters*, 10, 95-104.

Becerra, J.X. (1997). Insects on plants: Macroevolutionary chemical trends in host use. *Science*, 276, 253-256.

Becerra, J.X. (2007). The impact of herbivore-plant coevolution on plant community structure. *Proceedings of the National Academy of Sciences of the United States of America*, 104, 7483-7488.

Bivand, R.S. (2010). Exploratory spatial data analysis. In: *Handbook of applied spatial analysis*. Springer, pp. 219-254.

Blomberg, S.P., Garland Jr, T. & Ives, A.R. (2003). Testing for phylogenetic signal in comparative data: behavioral traits are more labile. *Evolution*, 57, 717-745.

Both, S., Riutta, T., Paine, C.E.T., Elias, D.M.O., Cruz, R.S., Jain, A. *et al.* (2019). Logging and soil nutrients independently explain plant trait expression in tropical forests. *New Phytologist*, 221, 1853-1865.

Burns, J.H. & Strauss, S.Y. (2011). More closely related species are more ecologically similar in an experimental test. *Proceedings of the National Academy of Sciences of the United States of America*, 108, 5302-5307.

Burton, J.I., Perakis, S.S., Brooks, J.R. & Puettmann, K.J. (2020). Trait integration and functional differentiation among co-existing plant species. *American Journal of Botany*, 107, 628-638.

Caldwell, E., Read, J. & Sanson, G.D. (2016). Which leaf mechanical traits correlate with insect herbivory among feeding guilds? *Annals of Botany*, 117, 349-361.

Cao, M., Zou, X.M., Warren, M. & Zhu, H. (2006). Tropical forests of Xishuangbanna, China. *Biotropica*, 38, 306-309.

Chesson, P. (2000). Mechanisms of maintenance of species diversity. *Annual Review of Ecology and Systematics*, 31, 343-366.

Chesson, P. & Kuang, J.J. (2008). The interaction between predation and competition. *Nature*, 456, 235-238.

Cheverud, J.M., Wagner, G.P. & Dow, M.M. (1989). Methods for the comparative analysis of variation patterns. *Systematic Biology*, 38, 201-213.

Coley, P.D. (1983). Herbivory and defensive characteristics of tree species in a lowland tropical forest. *Ecological Monographs*, 53, 209-234.

Condit, R., Ashton, P.S., Baker, P., Bunyavejchewin, S., Gunatilleke, S., Gunatilleke, N. *et al.* (2000). Spatial patterns in the distribution of tropical tree species. *Science*, 288, 1414-1418.

Condit, R., Engelbrecht, B.M.J., Pino, D., Perez, R. & Turner, B.L. (2013). Species distributions in response to individual soil nutrients and seasonal drought across a community of tropical trees. *Proceedings of the National Academy of Sciences of the United States of America*, 110, 5064-5068.

Connell, J.H. (1971). On the role of natural enemies in preventing competitive exclusion in some marine animals and in rain forest trees. *Dynamics of Populations*, 298, 312.

Davies, S.J., Palmiotto, P.A., Ashton, P.S., Lee, H.S. & Lafrankie, J.V. (1998). Comparative ecology of 11 sympatric species of *Macaranga* in Borneo: tree distribution in relation to horizontal and vertical resource heterogeneity. *Journal of Ecology*, 86, 662-673.

Ehrlich, P.R. & Raven, P.H. (1964). Butterflies and plants - a study in coevolution. *Evolution*, 18, 586-608.

Endara, M.J., Coley, P.D., Ghabash, G., Nicholls, J.A., Dexter, K.G., Donoso, D.A. *et al.* (2017). Coevolutionary arms race versus host defense chase in a tropical herbivore-plant system. *Proceedings of the National Academy of Sciences of the United States of America*, 114, E7499-E7505.

Erb, M. & Kliebenstein, D.J. (2020). Plant secondary metabolites as defenses, regulators, and primary metabolites: the blurred functional trichotomy. *Plant Physiology*, 184, 39-52.

Ernst, M., Grace, O.M., Saslis-Lagoudakis, C.H., Nilsson, N., Simonsen, H.T. & Rønsted, N. (2015). Global medicinal uses of *Euphorbia* L.(Euphorbiaceae). *Journal of Ethnopharmacology*, 176, 90-101.

Fine, P.V.A., Miller, Z.J., Mesones, I., Irazuzta, S., Appel, H.M., Stevens, M.H.H. *et al.* (2006). The growth–defense trade-off and habitat specialization by plants in amazonian forests. *Ecology*, 87, S150-S162.

Forrister, D.L., Endara, M.J., Younkin, G.C., Coley, P.D. & Kursar, T.A. (2019). Herbivores as drivers of negative density dependence in tropical forest saplings. *Science*, 363, 1213-1216.

Fortunel, C., Paine, C.E.T., Fine, P.V.A., Kraft, N.J.B. & Baraloto, C. (2014). Environmental factors predict community functional composition in Amazonian forests. *Journal of Ecology*, 102, 145-155.

Frazer, G.W., Canham, C. & Lertzman, K. (2000). Gap Light Analyzer (GLA), version 2.0. *Bulletin of the Ecological Society of America*, 81, 191-197.

Futuyma, D.J. & Moreno, G. (1988). The evolution of ecological specialization. *Annual review of Ecology and Systematics*, 19, 207-233.

Gause, G.F. (1934). The struggle for existence. *Williams and Wilkins, Baltimore.*

Gentry, A. (1989). Speciation in tropical forests. *Tropical forests: Botanical dynamics, speciation and diversity*, 113-134.

Gilbert, G.S. & Webb, C.O. (2007). Phylogenetic signal in plant pathogen-host range. *Proceedings of the National Academy of Sciences of the United States of America*, 104, 4979-4983.

Goslee, S.C. & Urban, D.L. (2007). The ecodist package for dissimilarity-based analysis of ecological data. *Journal of Statistical Software*, 22, 1-19.

Halpern, S.L., Adler, L.S. & Wink, M. (2010). Leaf herbivory and drought stress affect floral attractive and defensive traits in *Nicotiana quadrivalvis*. *Oecologia*, 163, 961-971.

Harvey, P.H. & Pagel, M. (1991). The comparative method in evolutionary biology. *Oxford University Press, Oxford*.

Holt, R.D. (1977). Predation, apparent competition, and the structure of prey communities. *Theoretical Population Biology*, 12, 197-229.

Janzen, D.H. (1970). Herbivores and the number of tree species in tropical forests. *The American Naturalist*, 104, 501-528.

Kembel, S.W. & Hubbell, S.P. (2006). The phylogenetic structure of a neotropical forest tree community. *Ecology*, 87, S86-S99.

Kembel, S.W., Cowan, P.D., Helmus, M.R., Cornwell, W.K., Morlon, H., Ackerly, D.D. *et al.* (2010). Picante: R tools for integrating phylogenies and ecology. *Bioinformatics*, 26, 1463-1464.

Kraft, N.J.B. & Ackerly, D.D. (2010). Functional trait and phylogenetic tests of community assembly across spatial scales in an Amazonian forest. *Ecological Monographs*, 80, 401-422.

Kurokawa, H. & Nakashizuka, T. (2008). Leaf herbivory and decomposability in a Malaysian tropical rain forest. *Ecology*, 89, 2645-2656.

Kursar, T.A. & Coley, P.D. (2003). Convergence in defense syndromes of young leaves in tropical rainforests. *Biochemical Systematics and Ecology*, 31, 929-949.

Kursar, T.A., Dexter, K.G., Lokvam, J., Pennington, R.T., Richardson, J.E., Weber, M.G. *et al.* (2009). The evolution of antiherbivore defenses and their contribution to species

coexistence in the tropical tree genus *Inga*. *Proceedings of the National Academy of Sciences of the United States of America*, 106, 18073-18078.

Labandeira, C.C., Wilf, P., Johnson, K.R. & Marsh, F. (2007). Guide to insect (and other) damage types on compressed plant fossils. *Smithsonian Institution, National Museum of Natural History, Department of Paleobiology, Washington, DC*.

Lan, G., Hu, Y., Cao, M., Zhu, H., Wang, H., Zhou, S. *et al.* (2008). Establishment of Xishuangbanna tropical forest dynamics plot: species compositions and spatial distribution patterns. *Zhiwu Shengtai Xuebao*, 32, 287-298.

Laughlin, D.C. & Messier, J. (2015). Fitness of multidimensional phenotypes in dynamic adaptive landscapes. *Trends in Ecology & Evolution*, 30, 487-496.

Le Bagousse-Pinguet, Y., Gross, N., Maestre, F.T., Maire, V., de Bello, F., Fonseca, C.R. *et al.* (2017). Testing the environmental filtering concept in global drylands. *Journal of Ecology*, 105, 1058-1069.

McKown, A.D., Akamine, M.E. & Sack, L. (2016). Trait convergence and diversification arising from a complex evolutionary history in Hawaiian species of *Scaevola*. *Oecologia*, 181, 1083-1100.

Messier, J., Lechowicz, M.J., McGill, B.J., Violle, C. & Enquist, B.J. (2017). Interspecific integration of trait dimensions at local scales: the plant phenotype as an integrated network. *Journal of Ecology*, 105, 1775-1790.

Münkemüller, T., Lavergne, S., Bzeznik, B., Dray, S., Jombart, T., Schiffers, K. *et al.* (2012). How to measure and test phylogenetic signal. *Methods in Ecology and Evolution*, 3, 743-756.

Novotny, V., Basset, Y., Miller, S.E., Weiblen, G.D., Bremer, B., Cizek, L. *et al.* (2002). Low host specificity of herbivorous insects in a tropical forest. *Nature*, 416, 841-844.

Ødegaard, F., Diserud, O.H. & Østbye, K. (2005). The importance of plant relatedness for host utilization among phytophagous insects. *Ecology Letters*, 8, 612-617.

Oksanen, J., Blanchet, F.G., Kindt, R., Legendre, P., Minchin, P., O'Hara, B. *et al.* (2015). Vegan: Community Ecology Package. *R Package Version 2.2-1*, 2, 1-2.

Pagare, S., Bhatia, M., Tripathi, N. & Bansal, Y.K. (2015). Secondary metabolites of plants and their role: Overview. *Current Trends in Biotechnology and Pharmacy*, 9, 293-304.

Palmer, M.W. (1994). Variation in species richness: towards a unification of hypotheses. *Folia Geobotanica et Phytotaxonomica*, 29, 511-530.

Rahman, A. & Akter, M. (2013). Taxonomy and medicinal uses of Euphorbiaceae (Spurge) family of Rajshahi, Bangladesh. *Research in Plant Sciences*, 1, 74-80.

Rasmann, S., Pellissier, L., Defossez, E., Jactel, H. & Kunstler, G. (2014). Climate-driven change in plant–insect interactions along elevation gradients. *Functional Ecology*, 28, 46-54.

Ravenscroft, C.H., Fridley, J.D. & Grime, J.P. (2014). Intraspecific functional differentiation suggests local adaptation to long-term climate change in a calcareous grassland. *Journal of Ecology*, 102, 65-73.

Ribeiro Jr, P. & Diggle, P. (2001). GeoR: A Package for Geostatistical Analysis. *R-NEWS*, 1, 14-18.

Ricotta, C. & Burrascano, S. (2008). Beta diversity for functional ecology. *Preslia*, 80, 61-72.

Rosas, T., Mencuccini, M., Barba, J., Cochard, H., Saura-Mas, S. & Martinez-Vilalta, J. (2019). Adjustments and coordination of hydraulic, leaf and stem traits along a water availability gradient. *New Phytologist*, 223, 632-646.

Rüger, N., Comita, L.S., Condit, R., Purves, D., Rosenbaum, B., Visser, M.D. *et al.* (2018). Beyond the fast–slow continuum: demographic dimensions structuring a tropical tree community. *Ecology Letters*, 21, 1075-1084.

Rüger, N., Condit, R., Dent, D.H., DeWalt, S.J., Hubbell, S.P., Lichstein, J.W. *et al.* (2020). Demographic trade-offs predict tropical forest dynamics. *Science*, 368, 165-168.

Salazar, D., Jaramillo, M.A. & Marquis, R.J. (2016). Chemical similarity and local community assembly in the species rich tropical genus *Piper*. *Ecology*, 97, 3176-3183.

Salazar, D., Lokvam, J., Mesones, I., Pilco, M.V., Zuniga, J.M.A., de Valpine, P. *et al.* (2018). Origin and maintenance of chemical diversity in a species-rich tropical tree lineage. *Nature Ecology & Evolution*, 2, 983-990.

Schemske, D.W., Mittelbach, G.G., Cornell, H.V., Sobel, J.M. & Roy, K. (2009). Is there a latitudinal gradient in the importance of biotic interactions? *Annual Review of Ecology, Evolution, and Systematics*, 40, 245-269.

Sedio, B.E., Wright, S.J. & Dick, C.W. (2012). Trait evolution and the coexistence of a species swarm in the tropical forest understorey. *Journal of Ecology*, 100, 1183-1193.

Sedio, B.E. & Ostling, A.M. (2013). How specialised must natural enemies be to facilitate coexistence among plants? *Ecology Letters*, 16, 995-1003.

Sedio, B.E. (2017). Recent breakthroughs in metabolomics promise to reveal the cryptic chemical traits that mediate plant community composition, character evolution and lineage diversification. *New Phytologist*, 214, 952-958.

Sedio, B.E., Boya P, C.A. & Rojas Echeverri, J.C. (2018a). A protocol for high-throughput, untargeted forest community metabolomics using mass spectrometry molecular networks. *Applications in Plant Sciences*, 6, e1033.

Sedio, B.E., Parker, J.D., McMahon, S.M. & Wright, S.J. (2018b). Comparative foliar metabolomics of a tropical and a temperate forest community. *Ecology*, 99, 2647-2653.

Sedio, B.E., Spasojevic, M.J., Myers, J.A., Wright, S.J., Person, M.D., Chandrasekaran, H. *et al.* (2021). Chemical similarity of co-occurring trees decreases with precipitation and temperature in North American forests. *Frontiers in Ecology and Evolution*, 9, 679638.

Sun, Y.R., Zhu, J.J., Sun, O.J. & Yan, Q.L. (2016). Photosynthetic and growth responses of *Pinus koraiensis* seedlings to canopy openness: implications for the restoration of mixed-broadleaved Korean pine forests. *Environmental and Experimental Botany*, 129, 118-126.

Swenson, N.G. (2011). The role of evolutionary processes in producing biodiversity patterns, and the interrelationships between taxonomic, functional and phylogenetic biodiversity. *American Journal of Botany*, 98, 472-480.

Trisos, C.H., Petchey, O.L. & Tobias, J.A. (2014). Unraveling the interplay of community assembly processes acting on multiple niche axes across spatial scales. *The American Naturalist*, 184, 593-608.

Vasas, A. & Hohmann, J. (2014). Euphorbia diterpenes: isolation, structure, biological activity, and synthesis (2008-2012). *Chemical Reviews*, 114, 8579-8612.

Vleminckx, J., Salazar, D., Fortunel, C., Mesones, I., Dávila, N., Lokvam, J. *et al.* (2018). Divergent secondary metabolites and habitat filtering both contribute to tree species coexistence in the Peruvian Amazon. *Frontiers in Plant Science*, 9, 836.

Volf, M., Laitila, J.E., Kim, J., Sam, L., Sam, K., Isua, B. *et al.* (2020). Compound specific trends of chemical defences in *Ficus* along an elevational gradient reflect a complex selective landscape. *Journal of Chemical Ecology*, 46, 442-454.

Volf, M., Segar, S.T., Miller, S.E., Isua, B., Sisol, M., Aubona, G. *et al.* (2018). Community structure of insect herbivores is driven by conservatism, escalation and divergence of defensive traits in *Ficus*. *Ecology Letters*, 21, 83-92.

Walker, J.B., Rinehart, S., Greenberg-Pines, G., White, W.K., DeSantiago, R., Lipson, D.A. *et al.* (2022). Aboveground competition influences density-dependent effects of cordgrass on sediment biogeochemistry. *Ecology and Evolution*, 12, e8722.

Westbrook, J.W., Kitajima, K., Burleigh, J.G., Kress, W.J., Erickson, D.L. & Wright, S.J. (2011). What makes a leaf tough? Patterns of correlated evolution between leaf

toughness traits and demographic rates among 197 shade-tolerant woody species in a neotropical forest. *American Naturalist*, 177, 800-811.

Wiens, J.J., Ackerly, D.D., Allen, A.P., Anacker, B.L., Buckley, L.B., Cornell, H.V. *et al.* (2010). Niche conservatism as an emerging principle in ecology and conservation biology. *Ecology Letters*, 13, 1310-1324.

Wink, M. (2018). Plant secondary metabolites modulate insect behavior-steps toward addiction? *Frontiers in Physiology*, 9, 364.

Wood, S.N. (2006). *Generalized additive models: an introduction with R*. chapman and hall/CRC.

Wright, I.J., Reich, P.B., Westoby, M., Ackerly, D.D., Baruch, Z., Bongers, F. *et al.* (2004). The worldwide leaf economics spectrum. *Nature*, 428, 821-827.

Yang, J., Zhang, G.C., Ci, X.Q., Swenson, N.G., Cao, M., Sha, L.Q. *et al.* (2014). Functional and phylogenetic assembly in a Chinese tropical tree community across size classes, spatial scales and habitats. *Functional Ecology*, 28, 520-529.

Yang, J., Swenson, N.G., Zhang, G.C., Ci, X.Q., Cao, M., Sha, L.Q. *et al.* (2015). Local-scale partitioning of functional and phylogenetic beta diversity in a tropical tree assemblage. *Scientific Reports*, 5.

Yang, J., Cao, M. & Swenson, N.G. (2018). Why functional traits do not predict tree demographic rates. *Trends in Ecology & Evolution*, 33, 326-336.

Yang, Y., Wang, H., Harrison, S.P., Prentice, I.C., Wright, I.J., Peng, C. *et al.* (2019). Quantifying leaf-trait covariation and its controls across climates and biomes. *New Phytologist*, 221, 155-168.

Yao, G.-Q., Nie, Z.-F., Turner, N.C., Li, F.-M., Gao, T.-P., Fang, X.-W. *et al.* (2021). Combined high leaf hydraulic safety and efficiency provides drought tolerance in *Caragana* species adapted to low mean annual precipitation. *New Phytologist*, 229, 230-244.

Zuur, A.F., Ieno, E.N. & Smith, G.M. (2007). *Analysing ecological data*. Springer, New York, USA.

TABLES

TABLE 1. Standardized *Mantel's* statistic (r_M) and associated *P*-value comparing empirical support for two hypotheses regarding the structure of phenotypic integration.

	r_M	*P*-value
Resource capture traits		
$H_{CENTRALITY}$	0.29	0.045
Correlated traits: C, N, LDMC, N:P		
H_{ALL}	0.44	0.002
Correlated traits: C, N, LDMC, N:P, C:N, Ca, Mg, dry mass, leaf area, SLA, fresh mass, P, K		
Photosynthetic traits		
$H_{CENTRALITY}$	0.64	0.002
Correlated traits: ST, CO, PT, R		
H_{ALL}	0.27	0.089
Correlated traits: ST, CO, PT, R, A_{max}, Ls, chlorophyll content, max height		
Hydraulic traits		
$H_{CENTRALITY}$	0.30	0.014
Correlated traits: C_{ft}^{*}, SWC, π_{tlp}, RWC,		
H_{ALL}	0.36	0.015
Correlated traits: C_{ft}^{*}, SWC, π_{tlp}, RWC, π_o, C_{ft}, C_{tlp}, ε, wood density, conductance, WUE		
Physical defensive traits		
$H_{CENTRALITY}$	0.34	0.040
Correlated traits: hemicellulose, thickness, toughness, ADL		
H_{ALL}	0.29	0.066
Correlated traits: hemicellulose, thickness, toughness, ADL, Si, cellulose, upper epidermal thickness, lower epidermal thickness		

Notes: $H_{CENTRALITY}$ – Centrality defined trait dimensions: only four traits with large degree value. H_{ALL} – All defined trait dimension: all traits in each dimension. For each trait dimension, the best supported hypothesis is highlighted in grey. Key to abbreviations: LDMC: leaf dry matter content; SLA: specific leaf area; ST: spongy tissue; CO: canopy openness; PT: palisade tissue; R: dark respiration; A_{max}: maximum photosynthetic rate; Ls: stomatal limitation; C_{ft}^{*}: absolute capacitance per leaf area at full turgor; SWC: saturated water content; π_{tlp}: turgor loss point; RWC: relative water content; π_o: saturated osmotic potential; C_{ft}: relative capacitance at full turgor; C_{tlp}: relative capacitance at turgor loss; ε: elasticity modulus; WUE: water use efficiency; ADL: acid detergent lignin.

FIGURE LEGENDS

FIGURE 1. The distribution of Euphorbiaceae tree species in the 20-ha Xishuangbanna seasonal tropical forest dynamics plot in China. A: The location of the 20-ha Xishuangbanna FDP; **B**: The distribution of Euphorbiaceae tree species in the plot; **C**: The pattern of all traits among 26 Euphorbiaceae species in five trait dimensions. In each trait dimension, the PC1 axis of all traits was used to represent the trait pattern. Abbreviations are: HY hydraulic traits; PH photosynthetic traits; PHY physical defensive traits; RE resource acquisition traits; SM secondary metabolites.

FIGURE 2. Network analysis of the relationship between traits and trait dimensions. Orange: resource acquisition traits; Blue: hydraulic traits; Green: physical defensive traits; Red: photosynthetic traits. Yellow dashed and solid green edges show negative and positive correlations, respectively. Only significant correlations ($r > 0.2$) are shown; line thickness reflects strength of correlation; the circle size indicates the degree value. See TABLE 1 for trait abbreviations.

FIGURE 3. Differentiation of traits with large centrality values and secondary metabolites with respect to environmental and spatial distance. Panels a-f illustrate distance decay of (A) photosynthetic traits with light environment and spatial distance, (B) hydraulic traits with soil water content and spatial distance, (C) resource acquisition traits with soil resource content and spatial distance, (D) physical defensive traits with average herbivory ratio and spatial distance, (E) secondary metabolites with average herbivory and spatial

distance, (F) all traits with all environmental and spatial distance. To calculate environmental distance with respect to soil variables and all variables, we used the first PC of variation in soil variables and in all traits, respectively. The contour lines represent the density of the traits and distance values.

FIGURE 4. Phylogenetic signal of functional traits in five trait dimensions. Panels illustrate relationships between phylogenetic distance and traits disparity with respect to **(A)** photosynthetic traits, **(B)** hydraulic traits, **(C)** resource acquisition traits, **(D)** physical defensive traits, and **(E)** secondary metabolites. Phylogenetic disparity with respect to the first component of variation in high-centrality traits is illustrated here, except for secondary metabolites for which we used 1-CSCS_{mrca} to represent phylogenetic disparity.

FIGURE 1.
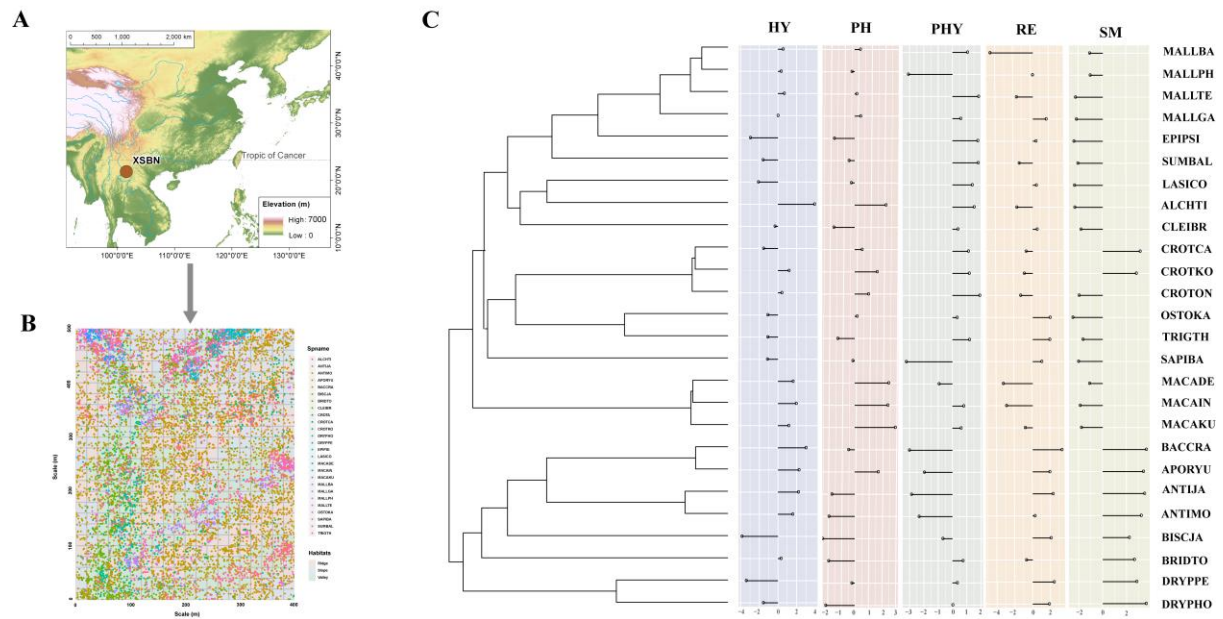
FIGURE 2.
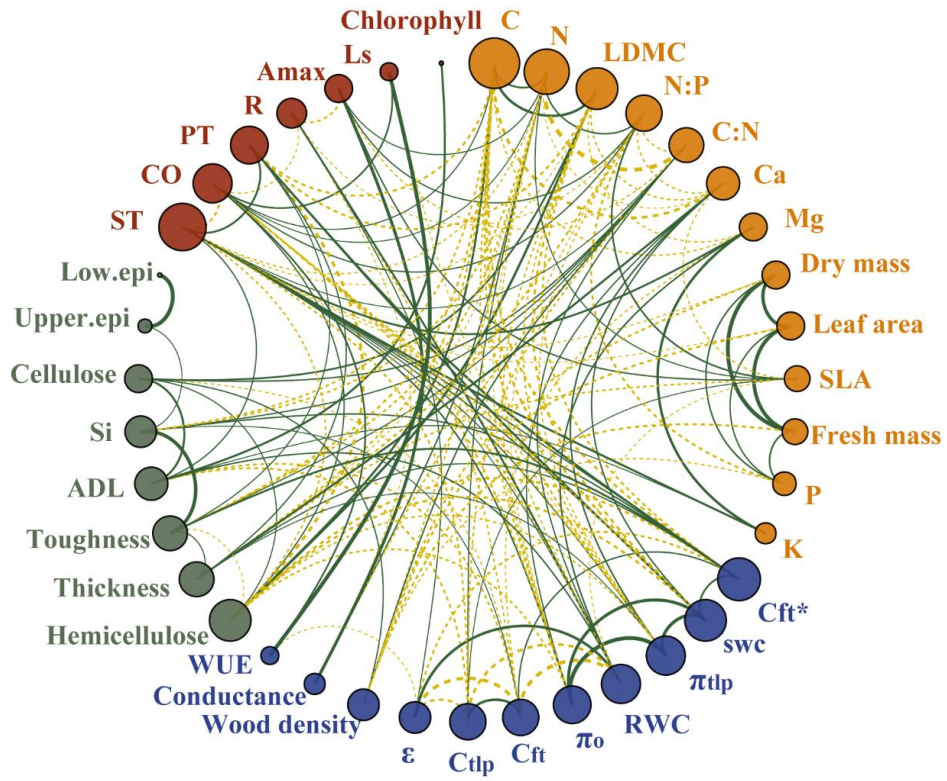
FIGURE 3.
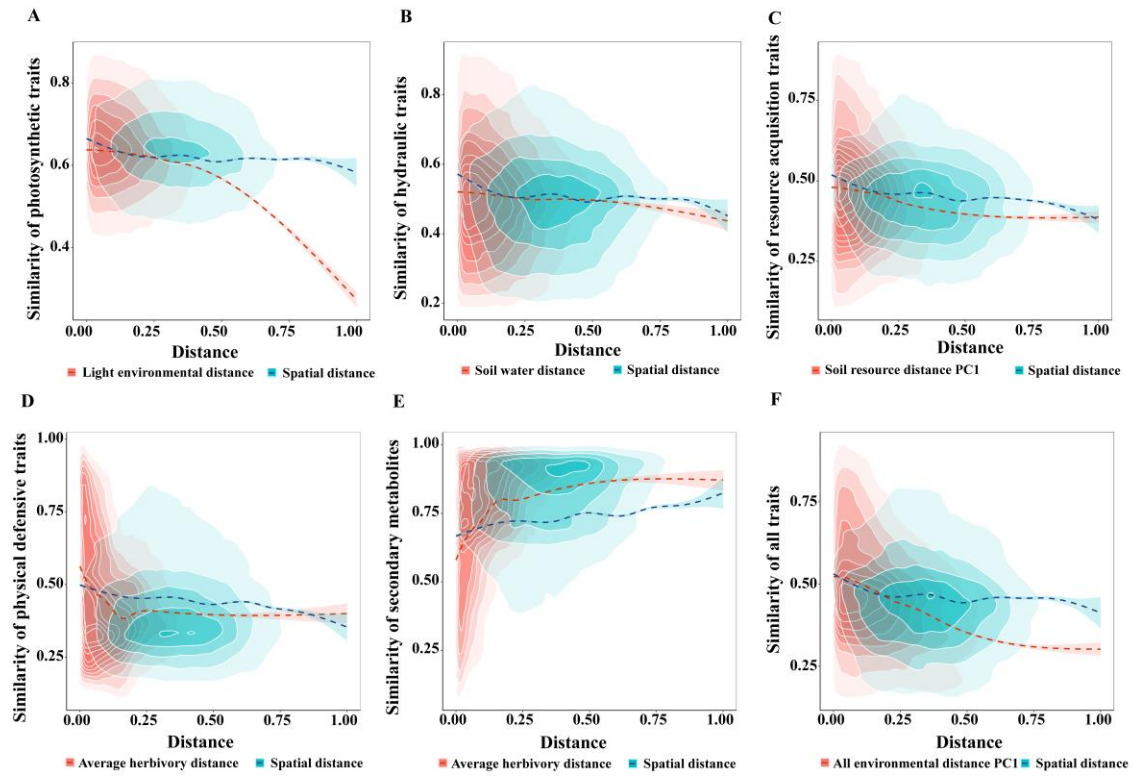
FIGURE 4.
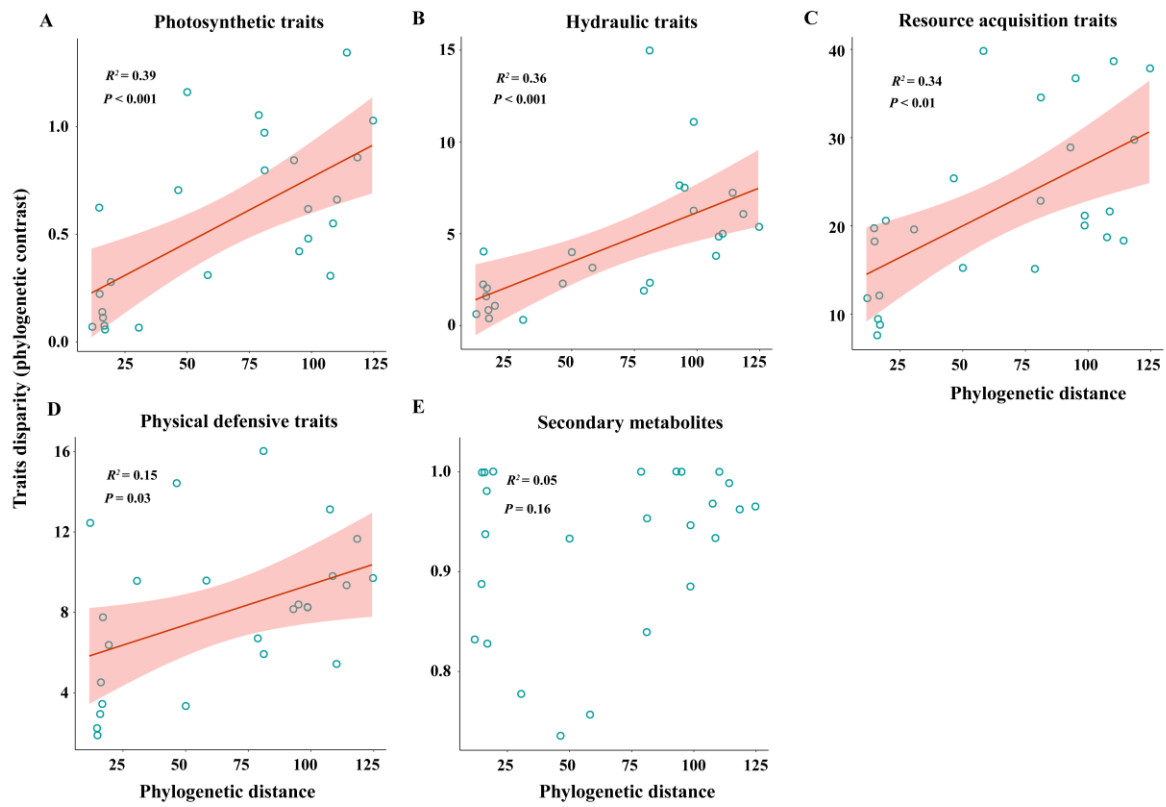
Supporting Information X.-Z., Wang, S.-W.,Sun, B. E. Sedio, S. Glomglieng, M. Cao, K.-F. Cao, J.-H., Yang, J.-L., Zhang, J. Yang. 2022.

Niche differentiation in both microhabitat and trophic interactions contributes to high local diversity of Euphorbiaceae in a tropical tree assemblage. Ecology Letters.

Appendix S1

Functional trait measurements

Appendix S2

TABLE S1-S12

FIGURE S1

Appendix S1

Functional trait measurements

Resource acquisition traits We collected 13 functional traits (TABLE S3), including: leaf area (LA), leaf fresh mass, leaf dry mass, specific leaf area (SLA), leaf dry matter content (LDMC), leaf total C content, leaf total N content, leaf total P content, leaf total K content, leaf total Ca content, leaf total Mg content, C and N ratio, and N and P ratio. For resource acquisition traits, we randomly collected 15 individuals for each species in the plot, and selected three to five healthy, undamaged leaves for each individual. Each leaf (without petiole or rachis) was scanned to measure LA by ImageJ software (Abramoff et al., 2004), then put the leaf in an envelope and placed them into an oven at 72 °C for 72 hours. Leaf mass and dry mass were measured by an electronic balance (AL204; Mettler Toledo Group, China). We then used the leaf area/leaf dry mass to calculate SLA and used leaf dry mass/fresh mass to calculate LDMC. Leaf carbon (C) and nitrogen (N) concentrations were measured with a Dumas-type combustion C-N elemental analyser (Vario MAX CN, Elementar Analysensysteme GmbH, Hanau, Germany), and phosphorus (P), potassium (K), calcium (Ca) and magnesium (Mg) concentrations were determined with an inductively coupled plasma atomic-emission spectrometer (iCAP6300, Thermo Fisher Scientific U.S.A). C/N ratio and N/P ratio were then calculated.

Photosynthetic traits We measured 8 photosynthetic traits (TABLE S3): max height, palisade tissue (PT), spongy tissue (ST), leaf maximum photosynthetic rate (Amax), dark respiration (R), stomatal limitation (LS), leaf chlorophyll content and canopy openness (CO). Six individuals with height ranging from 1 to 2.5 meters were randomly selected of each species

to determine photosynthetic gas exchange in relatively sunny and fully expanding leaves using LiCor Li-6400 portable photosynthetic apparatus (LI-6400, Lincoln, Nebraska, USA) with red/blue light sources. Then multiplied by SLA to convert into the net photosynthetic rate per unit leaf dry weight. Amax was measured from 9:30 a.m. to 11:30 a.m. every day at a light intensity of 1200 μmol m^{-2} s^{-1}. Small external CO_2 cylinders were used to reduce the influence of the fluctuation of understory environment which CO_2 concentration was set at 500 μmol mol^{-1}. R was measured between 20:30 p.m. and 22:30 p.m. CO_2 concentration inside the leaf (C_i) and the air CO_2 concentration (C_a) were both measured and based on that, we get L_S (L_S=1–C_i/C_a). We extracted chlorophyll contents with dimethylformamide according to the method of Porra et al. (1989) and quantified the content by spectrophotometry (UV 8000; Yuan Xi Co., Ltd., Shanghai, China). Two LAI 2000 plant canopy analyzers (LI-COR, Lincoln, Nebraska., USA) were used to quantify the light environment of Euphorbiaceae species. One was used to take measurements directly above each juvenile Euphorbiaceae species, and the other was placed above the seedlings. Comparing the data from the two instruments, the diffuse non-intercepted irradiance of the forest site can be estimated, which is equivalent to the canopy opening percentage (%CO) in the quasi-hemispherical field of view sensed by the LAI-2000 sensor (Lusk & Reich, 2000). Max tree height was measured according to the standard method of Cornelissen et al. (2003). We used a microscope (MD 2500; Leica Microsystems Ltd., Germany) to measure PT and ST for each individual.

Hydraulic traits We measured 11 hydraulic traits (TABLE S3): saturated water content (SWC), saturated osmotic potential (π_o), the turgor loss point (π_{tlp}), relative water content (RWC), elastic modulus (ε), relative capacitance at full turgor (C_{ft}), relative capacitance at

turgor loss (C_{tlp}), absolute capacitance per leaf area at full turgor (C_{ft}^*), water use efficiency (WUE), hydraulic conductance and wood density. Six individuals with height ranging from 1 to 2.5 meters were randomly selected with pedicels at least c. 1 cm long. At least 2 hours of shoots were rehydrated and equilibrated and initial water potentials measured. The initial water potentials were always higher than 0.15 MPa. Following the standard method, the bulk water potential is repeatedly measured by using a pressure chamber (0.01 MPa resolution; PMS Instruments, Albanay, OR, USA), and then the mass is measured to determine the relationship between the water potential and water content, thus generating pressure-volume curve for each sample (Scholander et al., 1965; Sack et al., 2010; Sack et al., 2011). Based on the pressure-volume curve, the standard method was used to calculate SWC, π_o, π_{tlp}, RWC, ε, C_{ft}, C_{tlp}, and C_{ft}^* (Bartlett et al. 2012a). Based on the measurements of A_{max} and stomatal conductance (g_s), WUE was then calculated as A_{max}/g_s (Cao et al., 2012). Hydraulic conductance was measured using the vacuum chamber technique (Kolb et al. 1996). Wood samples were taken from large branches using a tree borer (RESISTOGRAPHY, Rinntech Co., Germany), and wood density was measured by water displacement method (Chave, 2005).

Physical defensive traits We measured 8 physical defensive traits (TABLE S3), including: leaf toughness, leaf thickness, upper epidermal thickness (upper.epi), lower epidermal thickness (lower.epi), leaf silicon content (Si), acid detergent lignin (ADL), hemicellulose and cellulose content. For physical defensive traits, we randomly collected 15 individuals for each species in the plot, and selected three to five healthy, undamaged leaves for each individual. Leaf toughness was measured as the force necessary for penetrating the leaf using an Imada PS-2N push/pull mechanical force gauge with a 5 mm diameter blunt tip (Imada, Inc.,

Northbrook, Illinois). Leaf thickness was measured using a vernier caliper. We used a microscope (MD 2500; Leica Microsystems Ltd., Germany) to measure thickness of the upper epidermal and lower epidermal layers. In our study, we measured Si content according to the national standard method in which samples were digested with nitric acid-perchloric acid (LY/T 1270-1999). We used a fiber analyzer (Fibertec TM 2010, FOSS Analytical AB) to measure acid detergent fiber (ADF), acid detergent lignin (ADL) and neutral detergent fiber content (NDF) by the gravimetric method (NY/T 1459-2007; GB/T 2080-2006). We used these measurements to calculate hemicellulose content (NDF-ADF) and cellulose content (ADF-ADL).

Secondary metabolites Plants rely on a large number of secondary metabolites to resist pathogens and herbivores (Richards et al., 2015). We randomly selected over five individuals for each species, collected three expanding, unlignified leaves from each individual and stored them at −80 °C in the laboratory within three hours. Secondary metabolites in leaves were extracted and analyzed following Sedio et al. (2018) with slight modification. Briefly, we weighed 110 mg leaf tissue and fully ground it to a fine powder, then fully extracted small molecules of a wide range in polarity using 700 μL 90:10 methanol: water at pH 4.5 for 10 min. Mild acidity improves the extraction of alkaloids. We analyzed extracted samples by ultra-high performance liquid chromatography-tandem mass spectrometry (UHPLC-MS/MS; Agilent 1260 UPLC/Q-TOF, USA).

We analyzed the UHPLC-MS/MS data using the Global Natural Products Social (GNPS) Molecular Networking metabolomics tool (Wang et al., 2016). Molecular networks rely on the observation that structurally similar molecules break into many of the same sub-structures.

Thus, a comparison of the mass to charge ratio (m/z) of the fragments of two molecules reflects their structural similarity. The comparison of MS/MS spectra for many pairs of compounds can therefore be used to generate a molecular network in which nodes represent unique features or compounds, and links reflect structural similarity.

We created a molecular network using the "metabolomics-snets-v2" online workflow (https://ccms-ucsd.github.io/GNPSDocumentation/) on the GNPS website (http://gnps.ucsd.edu). The data were filtered by removing all MS/MS fragment ions within +/-17 Da of the precursor m/z. MS/MS spectra were window filtered by choosing only the top 6 fragment ions in the +/- 50Da window throughout the spectrum. The precursor ion mass tolerance was set to 1.0 Da and a MS/MS fragment ion tolerance of 0.5 Da. A network was then created where edges were filtered to have a cosine score above 0.6 and more than 3 matched peaks. Further, edges between two nodes were kept in the network if and only if each of the nodes appeared in each other's respective top 10 most similar nodes. Finally, the maximum size of a molecular family was set to 0, and the lowest scoring edges were removed from molecular families until the molecular family size was below this threshold. The spectra in the network were then searched against GNPS spectral libraries. The library spectra were filtered in the same manner as the input data. All matches kept between network spectra and library spectra were required to have a score above 0.6 and at least 6 matched peaks (Wang et al., 2016). Our molecular network and associated MS data can be found at http://gnps.ucsd.edu/ProteoSAFe/status.jsp?task=1c27b5d80c314733962cb5c759b43f27. In order to compare metabolites among species, we calculated a metric that quantifies all pairwise combinations of compounds to calculate the chemical structural and compositional similarity

(CSCS) scores for each pairwise combination of all 26 species following Sedio et al. (2017).

Appendix S2

TABLE S1. Euphorbiaceae species list

Species	Spname
Sumbaviopsis albicans	SUMBAL
Epiprinus siletianus	EPIPSI
Mallotus garrettii	MALLGA
Mallotus tetracoccus	MALLTE
Mallotus philippensis	MALLPH
Mallotus barbatus	MALLBA
Cleidion brevipetiolatum	CLEIBR
Alchornea tiliifolia	ALCHTI
Lasiococca comberi	LASICO
Sapium baccatum	SAPIBA
Trigonostemon thyrsoideus	TRIGTH
Ostodes katharinae	OSTOKA
Croton tiglium	CROTON
Croton kongensis	CROTKO
Croton cascarilloides	CROTCA
Macaranga kurzii	MACAKU
Macaranga indica	MACAIN
Macaranga denticulata	MACADE
Bridelia tomentosa	BRIDTO
Antidesma montanum	ANTIMO
Antidesma japonicum	ANTIJA
Aporusa yunnanensis	APORYU
Baccaurea ramiflora	BACCRA
Bischofia javanica	BISCJA
Drypetes hoaensis	DRYPHO
Drypetes perreticulata	DRYPPE

Note: The Euphorbiaceae in this study was collected based on APG III phylogenetic tree.

TABLE S2. Functional traits, ecological strategies and functional dimension.

Functional traits	Ecological strategy
Secondary metabolite	Anti-bacteria, and could cause susceptibility to both specialist and generalist herbivores (Moore et al., 2014; Speed et al., 2015).
Acid detergent lignin (ADL)	Increase leaf toughness and can also affect insect feeding and digestion (Choong, 1996; Kula et al., 2020).
Hemicellulose content	
Cellulose content	
Silicon content (Si)	Reduce leaf consumption and have negative impacts on herbivores (Debona et al., 2017)
Leaf toughness	
Leaf thickness	Important physical leaf attributes affecting food selection by leaf-eating insects (Kitajima et al., 2012).
Upper Epidermal thickness	
Lower Epidermal thickness	
Total C	
Total N	
Total P	
Total K	Ascertain resource use strategies and the contents that these can reflect in resource availability (Vrede et al., 2004; Reich, 2014).
Total Ca	
Total Mg	
C:N	
N:P	
Specific leaf area (SLA)	
Leaf dry matter content (LDMC)	Reflects the ability of plants to acquire resources (Wright et al., 2004).
Leaf area (LA)	
Fresh mass	It is an important index for efficient resource use, could reflect trade-off between resources used for growth and resistance to pests and diseases (Cornelissen et al., 2003).
Dry mass	

Max height	Taller plants are benefits for photosynthesis (Poorter et al., 2005).
Palisade tissue (PT)	
Spongy tissue (ST)	Leaf structures, related to photosynthetic rate (James & Bell, 2000).
Dark respiration (R)	
Maximum photosynthetic rate (A_{max})	It reflects the photosynthetic characteristics of plants (Smith & Dukes, 2013; Li et al., 2016).
Stomatal limitation (Ls)	It is the main limiting factor to determine photosynthesis of plants under certain water stress (Drake et al., 2017).
Canopy openness (CO)	The greater the canopy opening, much light from the upper canopy into the understory (Alvarez-Yepiz et al., 2014).
Leaf chlorophyll content	Related to photosynthetic rate (Sims & Gamon, 2002; Croft et al., 2017).
Water use efficiency (WUE)	Reflects the water consumption and drought resistance of trees (Liu et al., 2015).
Conductance	It is the most sensitive index of water content (Li et al., 2020).
Saturated water content (swc)	Reflects the plant response to drought environment (Bartlett et al., 2012a).
Saturated osmotic potential (π_o)	Strategies of plants to respond to drought environments (Lau & Young, 1988).
Turgor loss point (π_{tlp})	
Relative capacitance at full turgor (C_{ft})	
Relative capacitance at turgor loss (C_{tlp})	Index to quantify the ability of plants to tolerate drought (Bartlett et al., 2012b).
Relative water content (RWC)	
Absolute capacitance per leaf area at full turgor (C_{ft}^{*})	
Elasticity Modulus (ε)	An indicator of drought tolerance of plants (Lo Gullo & Salleo, 1988).
Wood density	Related to ε, and also enables increased tolerance to water stress (Lawson et al., 2015).

TABLE S3. Functional traits and categories.

Functional traits	Units	Ecological strategy
Secondary metabolite		Chemical defence
Acid detergent lignin (ADL)	%	Physical defence
Hemicellulose content	%	Physical defence
Cellulose content	%	Physical defence
Silicon content (Si)	$g \cdot kg^{-1}$	Physical defence
Leaf toughness	mm	Physical defence
Leaf thickness	mm	Physical defence
Upper Epidermal thickness	μm	Physical defence
Lower Epidermal thickness	μm	Physical defence
Total C	$g \cdot kg^{-1}$	Resource acquisition
Total N	$g \cdot kg^{-1}$	Resource acquisition
Total P	$g \cdot kg^{-1}$	Resource acquisition
Total K	$g \cdot kg^{-1}$	Resource acquisition
Total Ca	$g \cdot kg^{-1}$	Resource acquisition
Total Mg	$g \cdot kg^{-1}$	Resource acquisition
C:N		Resource acquisition
N:P		Resource acquisition
Specific leaf area (SLA)	$cm^2 \cdot g^{-1}$	Resource acquisition
Leaf dry matter content (LDMC)	$mg \cdot g{-1}$	Resource acquisition
Leaf area (LA)	cm^2	Resource acquisition
Fresh mass	g	Resource acquisition
Dry mass	g	Resource acquisition
Max height	m	Photosynthetic
Palisade tissue (PT)	μm	Photosynthetic
Spongy tissue (ST)	μm	Photosynthetic
Dark respiration (R)	$nmol \cdot g^{-1} \cdot s^{-1}$	Photosynthetic
Maximum photosynthetic rate (A_{max})	$nmol \cdot g^{-1} \cdot s^{-1}$	Photosynthetic
Stomatal limitation (Ls)	%	Photosynthetic
Canopy openness (CO)	%	Photosynthetic
Leaf chlorophyll content	$μg \cdot cm^{-2}$	Photosynthetic
Water use efficiency (WUE)	$μmol \cdot mol^{-1}$	Hydraulic
Conductance	$mol \cdot m^2 \cdot s^{-1}$	Hydraulic
Saturated water content (swc)	%	Hydraulic
Saturated osmotic potential (π_o)	MPa	Hydraulic
Turgor loss point (π_{tlp})	MPa	Hydraulic
Relative capacitance at full turgor (C_{ft})	MPa^{-1}	Hydraulic
Relative capacitance at turgor loss (C_{tlp})	MPa^{-1}	Hydraulic

Relative water content (RWC)	%	Hydraulic
Absolute capacitance per leaf area at full turgor (C_{ft}^{*})	$mol \cdot m^{-2} \cdot MPa^{-1}$	Hydraulic
Elasticity Modulus (ε)	MPa	Hydraulic
Wood density	$g \cdot cm^{-3}$	Hydraulic

TABLE S4. Descriptive statistics of 40 functional traits.

	Mean	Min	Max	Variance	Standard deviation
Acid detergent lignin (ADL)	14.122	5.520	27.610	35.413	5.951
Hemicellulose content	12.665	4.030	19.700	17.835	4.223
Cellulose content	21.422	8.990	32.970	38.521	6.207
Silicon content (Si)	4.895	0.150	16.020	16.530	4.066
Leaf toughness	0.170	0.103	0.317	0.002	0.048
Leaf thickness	0.788	0.209	1.909	0.215	0.464
Upper Epidermal thickness	0.012	0.003	0.050	0.000	0.012
Lower Epidermal thickness	0.010	0.003	0.049	0.000	0.011
Total C	463.077	398.000	503.000	602.074	24.537
Total N	24.276	16.010	31.140	19.390	4.403
Total P	19.608	15.254	25.244	10.153	3.186
Total K	15.570	9.553	22.081	10.767	3.281
Total Ca	1.600	1.100	2.570	0.116	0.340
Total Mg	15.002	6.370	32.410	41.966	6.478
C:N	11.945	4.180	21.530	23.784	4.877
N:P	4.178	1.800	11.480	4.281	2.069
Specific leaf area (SLA)	165.288	68.588	255.892	1958.941	44.260
Leaf dry matter content (LDMC)	2.820	0.440	11.915	8.753	2.959
Leaf area (LA)	0.880	0.190	4.079	0.929	0.964
Fresh mass	131.612	27.055	633.542	16920.280	130.078
Dry mass	0.324	0.222	0.457	0.005	0.071
Max height	49.938	34.234	63.911	55.799	7.470
Palisade tissue (PT)	0.019	0.009	0.046	0.000	0.009
Spongy tissue (ST)	0.037	0.006	0.094	0.001	0.024
Dark respiration (R)	-0.510	-0.669	-0.361	0.006	0.075
Maximum photosynthetic rate (A_{max})	8.733	5.779	13.700	3.469	1.863
Stomatal limitation (Ls)	0.231	0.182	0.275	0.001	0.027
Canopy openness (CO)	12.731	4.000	40.000	55.005	7.417
Leaf chlorophyll content	2.666	1.353	4.124	0.562	0.750

Water use efficiency (WUE)	61.955	48.527	77.349	63.131	7.945
Conductance	0.150	0.092	0.214	0.001	0.034
Saturated water content (swc)	2.912	1.525	5.016	1.004	1.002
Saturated osmotic potential (π_o)	-1.484	-2.174	-0.865	0.102	0.319
Turgor loss point (π_{tlp})	-1.724	-2.350	-1.051	0.116	0.340
Relative capacitance at full turgor (C_{ft})	89.520	76.446	97.486	21.041	4.587
Relative capacitance at turgor loss (C_{tlp})	17.883	9.567	29.717	31.705	5.631
Relative water content (RWC)	0.060	0.021	0.102	0.000	0.020
Absolute capacitance per leaf area at full turgor (Cft*)	0.308	0.089	0.530	0.012	0.110
Elasticity Modulus (ε)	0.466	0.157	1.232	0.091	0.301
Wood density	0.555	0.345	0.749	0.011	0.103

TABLE S5. Explanation of Principal Component Analysis on soil variables.

Soil nutrients	PCA1	PCA2	PCA3
AN	0.902	-0.33	0.116
AP	0.773	0.343	-0.534
AK	0.629	0.676	0.382
C	0.851	-0.461	0.08
Eigenvalue	2.531	0.896	0.451
% explained	63.268	22.4	11.283

TABLE S6. Explanation of Principal Component Analysis on all environmental variables.

All env	PCA1	PCA2	PCA3
Water	-0.516	0.231	0.513
CO	0.521	-0.175	-0.448
Soil.pc1	0.297	0.573	-0.141
Soil.pc2	0.491	0.091	-0.081
Soil.pc3	-0.185	0.412	0.602
Ave.herb	0.779	0.117	-0.037
Hole.ratio	0.010	-0.762	0.0106
Marginal.ratio	0.866	0.325	0.007
Gen.ratio	-0.627	0.580	-0.420
Inter.ratio	0.694	-0.456	0.455
Speci.ratio	-0.708	-0.545	-0.190
Eigenvalue	3.634	2.131	1.274
% explained	33.036	19.376	11.582

Note: ave.herb means: average herbivory ratio; gen.ratio: generalized ratio; inter.ratio: intermediated ratio; speci.ratio: specialized ratio.

TABLE S7. Trait network centrality.

Traits	Degree	Functional dimension
ST	22	Ph
CO	15	Ph
PT	14	Ph
R	9	Ph
A_{max}	8	Ph
Ls	4	Ph
Chlorophyll	2	Ph
Cft[*]	18	Hy
swc	17	Hy
π_{tlp}	15	Hy
RWC	15	Hy
π_o	14	Hy
C_{ft}	13	Hy
C_{tlp}	13	Hy
Elasticity modulus	10	Hy
Wood density	10	Hy
Conductance	5	Hy
WUE	4	Hy
C	25	Re
N	20	Re
LDMC	17	Re
N:P	13	Re
C:N	12	Re
Ca	11	Re
Mg	8	Re
Dry mass	8	Re
Leaf area	8	Re
SLA	7	Re
Fresh mass	7	Re
P	6	Re
K	5	Re
Hemicellulose	17	Phy
Thickness	12	Phy
Toughness	12	Phy
ADL	11	Phy
Si	10	Phy
Cellulose	8	Phy
Upper.epi	3	Phy
Lower.epi	2	Phy

Notes: The centrality value reported is 'degree value'. Ph: photosynthetic traits; Phy: physical defensive traits; Re: resource acquisition traits; SM: secondary metabolites; Hy: hydraulic traits. See TABLE S3 and texts for trait abbreviations. The traits in bold represent the centrality traits.

TABLE S8. Hypothesis and data matrices for the resource acquisition traits

	C	N	C:N	N:P	P	K	Ca	Mg	SLA	fresh mass	dry mass	leaf area	LDMC
S8A. Hypothesis matrix for centrality trait dimensions													
C	1	1	0	1	0	-	-	-	0	0	0	0	1
N	1	1	0	1	0	-	-	-	0	0	0	0	1
C:N	0	0	1	0	0	-	-	-	0	0	0	0	0
N:P	1	1	0	1	0	-	-	-	0	0	0	0	1
P	0	0	0	0	1	-	-	-	0	0	0	0	0
K	-	-	-	-	-	1	-	-	-	-	-	-	-
Ca	-	-	-	-	-	-	1	-	-	-	-	-	-
Mg	-	-	-	-	-	-	-	1	-	-	-	-	-
SLA	0	0	0	0	0	-	-	-	1	-	-	0	0
fresh mass	0	0	0	0	0	-	-	-	-	1	0	0	0
dry mass	0	0	0	0	0	-	-	-	-	0	1	0	0
leaf area	0	0	0	0	0	-	-	-	0	0	0	1	0
LDMC	1	1	0	1	0	-	-	-	0	0	0	0	1
S8B. Hypothesis matrix for all traits													
C	1	1	1	1	1	-	-	-	-1	-1	-1	-1	1
N	1	1	-1	1	-1	-	-	-	1	-1	-1	1	1
C:N	1	-1	1	-1	-1	-	-	-	-1	-1	-1	-1	1
N:P	1	1	-1	1	-1	-	-	-	1	1	1	1	1
P	1	-1	-1	-1	1	-	-	-	-1	-1	-1	1	-1
K	-	-	-	-	-	1	-	-	-	-	-	-	-
Ca	-	-	-	-	-	-	1	-	-	-	-	-	-
Mg	-	-	-	-	-	-	-	1	-	-	-	-	-
SLA	-1	1	-1	1	-1	-	-	-	1	-	-	1	-1
fresh mass	-1	-1	-1	1	-1	-	-	-	-	1	1	1	-1
dry mass	-1	-1	-1	1	-1	-	-	-	-	1	1	1	1
leaf area	-1	1	-1	1	1	-	-	-	1	1	1	1	-1
LDMC	1	1	1	1	-1	-	-	-	-1	-1	1	-1	1
S8C. Observed correlation matrix for resource capture traits													
C	1.00	0.55	-0.32	0.35	0.11	-0.06	-0.75	-0.48	0.17	0.09	0.19	0.18	0.68
N	0.55	1.00	-0.96	0.51	0.36	0.14	-0.40	-0.32	0.41	0.24	0.28	0.38	0.14
C:N	-0.32	-0.96	1.00	-0.47	-0.38	-0.17	0.19	0.19	-0.39	-0.27	-0.28	-0.38	0.06
N:P	0.35	0.51	-0.47	1.00	-0.60	-0.04	-0.48	-0.22	0.53	-0.31	-0.25	-0.15	0.17
P	0.11	0.36	-0.38	-0.60	1.00	0.19	0.19	-0.02	-0.20	0.53	0.50	0.48	-0.09
K	-0.06	0.14	-0.17	-0.04	0.19	1.00	-0.13	0.70	0.16	-0.09	-0.16	-0.10	-0.28
Ca	-0.75	-0.40	0.19	-0.48	0.19	-0.13	1.00	0.38	-0.45	0.25	0.18	0.12	-0.50
Mg	-0.48	-0.32	0.19	-0.22	-0.02	0.70	0.38	1.00	-0.07	-0.11	-0.21	-0.17	-0.43
SLA	0.17	0.41	-0.39	0.53	-0.20	0.16	-0.45	-0.07	1.00	-0.30	-0.34	0.02	0.01

fresh mass	0.09	0.24	-0.27	-0.31	0.53	-0.09	0.25	-0.11	-0.30	1.00	0.98	0.90	-0.16
dry mass	0.19	0.28	-0.28	-0.25	0.50	-0.16	0.18	-0.21	-0.34	0.98	1.00	0.85	0.00
leaf area	0.18	0.38	-0.38	-0.15	0.48	-0.10	0.12	-0.17	0.02	0.90	0.85	1.00	-0.10
LDMC	0.68	0.14	0.06	0.17	-0.09	-0.28	-0.50	-0.43	0.01	-0.16	0.00	-0.10	1.00

TABLE S9. Hypothesis and data matrices for the photosynthetic traits

	chlorophyll	PT	ST	R	A_{max}	Ls	max height	CO
S9A. Hypothesis matrix for centrality trait dimensions								
chlorophyll	1	0	0	0	0	0	0	0
PT	0	1	1	-1	0	0	0	-1
ST	0	1	1	1	0	0	0	-1
R	0	-1	1	1	0	0	0	-1
A_{max}	0	0	0	0	1	0	0	0
Ls	0	0	0	0	0	1	0	0
max height	0	0	0	0	0	0	1	0
CO	0	-1	-1	-1	0	0	0	1
S9B. Hypothesis matrix for all traits								
chlorophyll	1	-1	-1	1	1	-1	-1	-1
PT	-1	1	1	-1	1	-1	1	-1
ST	-1	1	1	1	-1	-1	1	-1
R	1	-1	1	1	1	-1	-1	-1
A_{max}	1	1	-1	1	1	-1	1	1
Ls	-1	-1	-1	-1	-1	1	1	-1
max height	-1	1	1	-1	1	-1	1	1
CO	-1	-1	-1	-1	1	-1	1	1
S9C. Observed correlation matrix for photosynthetic traits								
chlorophyll	1.00	0.01	0.19	0.19	-0.02	0.02	-0.34	-0.15
PT	0.01	1.00	0.58	-0.25	0.37	0.20	0.09	-0.38
ST	0.19	0.58	1.00	0.27	-0.02	0.10	0.04	-0.58
R	0.19	-0.25	0.27	1.00	-0.56	-0.23	-0.04	-0.42
A_{max}	-0.02	0.37	-0.02	-0.56	1.00	0.28	-0.13	0.22
Ls	0.02	0.20	0.10	-0.23	0.28	1.00	-0.33	0.53
max height	-0.34	0.09	0.04	-0.04	-0.13	-0.33	1.00	-0.16
CO	-0.15	-0.38	-0.58	-0.42	0.22	0.53	-0.16	1.00

TABLE S10. Hypothesis and data matrices for the hydraulic traits

	WUE	conductance	swc	π_o	π_{tlp}	RWC	elasticity modulus	C_{ft}	C_{tlp}	C_{ft}^*	wood density
S10A. Hypothesis matrix for centrality trait dimensions											
WUE	1	0	0	0	0	0	0	0	0	0	0
conductance	0	1	0	0	0	0	0	0	0	0	0
swc	0	0	1	0	1	-1	0	0	0	1	0
π_o	0	0	0	1	0	0	0	0	0	0	0
π_{tlp}	0	0	1	0	1	1	0	0	0	1	0
RWC	0	0	-1	0	1	1	0	0	0	-1	0
elasticity modulus	0	0	0	0	0	0	1	0	0	0	0
C_{ft}	0	0	0	0	0	0	0	1	0	0	0
C_{tlp}	0	0	0	0	0	0	0	0	1	0	0
C_{ft}^*	0	0	1	0	1	-1	0	0	0	1	0
wood density	0	0	0	0	0	0	0	0	0	0	1
S10B. Hypothesis matrix for all traits											
WUE	1	-1	1	-1	-1	-1	1	-1	-1	-1	1
conductance	-1	1	-1	1	1	-1	1	1	1	1	1
swc	1	-1	1	1	1	-1	-1	1	1	1	-1
π_o	-1	1	1	1	1	-1	-1	1	1	1	-1
π_{tlp}	-1	1	1	1	1	1	-1	1	1	1	-1
RWC	-1	-1	-1	-1	1	1	-1	-1	1	-1	-1
elasticity modulus	1	1	-1	-1	-1	-1	1	-1	-1	-1	1
C_{ft}	-1	1	1	1	1	-1	-1	1	1	1	-1
C_{tlp}	-1	1	1	1	1	1	-1	1	1	1	-1
C_{ft}^*	-1	1	1	1	1	-1	-1	1	1	1	-1
wood density	1	1	-1	-1	-1	-1	1	-1	-1	-1	1
S10C. Observed correlation matrix for hydraulic traits											
WUE	1.00	-0.35	-0.16	-0.30	-0.31	-0.34	-0.40	0.23	0.12	0.25	-0.16
conductance	-0.35	1.00	0.37	0.20	0.21	-0.05	-0.12	0.16	0.24	-0.01	-0.36
swc	-0.16	0.37	1.00	0.81	0.82	0.16	-0.24	0.17	0.00	0.56	-0.08
π_o	-0.30	0.20	0.81	1.00	0.97	0.36	-0.16	0.04	-0.24	0.33	0.02
π_{tlp}	-0.31	0.21	0.82	0.97	1.00	0.37	-0.15	0.01	-0.15	0.27	0.01
RWC	-0.34	-0.05	0.16	0.36	0.37	1.00	0.72	-0.85	-0.71	-0.32	0.16
elasticity modulus	-0.40	-0.12	-0.24	-0.16	-0.15	0.72	1.00	-0.84	-0.65	-0.57	0.25
C_{ft}	0.23	0.16	0.17	0.04	0.01	-0.85	-0.84	1.00	0.68	0.48	-0.31
C_{tlp}	0.12	0.24	0.00	-0.24	-0.15	-0.71	-0.65	0.68	1.00	0.24	-0.28
C_{ft}^*	0.25	-0.01	0.56	0.33	0.27	-0.32	-0.57	0.48	0.24	1.00	0.01
wood density	-0.16	-0.36	-0.08	0.02	0.01	0.16	0.25	-0.31	-0.28	0.01	1.00

TABLE S11. Hypothesis and data matrices for the physical defensive traits

	ADL	hemicellulose	cellulose	Si	thickness	toughness	upper.epi	lower.epi
S11A. Hypothesis matrix for centrality trait dimensions								
ADL	1	-1	0	0	1	-1	0	0
hemicellulose	-1	1	0	0	-1	-1	0	0
cellulose	0	0	1	0	0	0	0	0
Si	0	0	0	1	0	0	0	0
thickness	1	-1	0	0	1	1	0	0
toughness	-1	-1	0	0	1	1	0	0
upper.epi	0	0	0	0	0	0	1	0
lower.epi	0	0	0	0	0	0	0	1
S11B. Hypothesis matrix for all traits								
ADL	1	-1	1	1	1	-1	1	1
hemicellulose	-1	1	-1	1	-1	-1	1	1
cellulose	1	-1	1	-1	-1	-1	1	1
Si	1	1	-1	1	1	1	1	1
thickness	1	-1	-1	1	1	1	1	1
toughness	-1	-1	-1	1	1	1	1	1
upper.epi	1	1	1	1	1	1	1	1
lower.epi	1	1	1	1	1	1	1	1
S11C. Observed correlation matrix for physical defensive traits								
ADL	1.00	0.05	0.60	-0.28	0.06	-0.12	-0.06	-0.02
hemicellulose	0.05	1.00	0.41	-0.33	-0.31	-0.40	-0.17	-0.06
cellulose	0.60	0.41	1.00	-0.05	0.05	0.01	0.01	0.05
Si	-0.28	-0.33	-0.05	1.00	0.17	0.89	0.40	0.30
thickness	0.06	-0.31	0.05	0.17	1.00	0.41	-0.03	-0.16
toughness	-0.12	-0.40	0.01	0.89	0.41	1.00	0.33	0.21
upper.epi	-0.06	-0.17	0.01	0.40	-0.03	0.33	1.00	0.98
lower.epi	-0.02	-0.06	0.05	0.30	-0.16	0.21	0.98	1.00

TABLE S12. Phylogenetic signal of four large centrality traits examined using K value of the

Brownian Motion evolutionary model test.

Functional traits dimensions	PCA axis	K	t-value	P-value
	PCA1	**1.423**	−	**0.001**
Photosynthetic traits	PCA2	0.389	−	0.358
	PCA3	**0.754**	−	**0.002**
	PCA1	**0.870**	−	**0.001**
Hydraulic traits	PCA2	**0.922**	−	**0.001**
	PCA3	**0.848**	−	**0.001**
	PCA1	**0.742**	−	**0.004**
Resource acquisition traits	PCA2	0.526	−	0.065
	PCA3	0.293	−	0.680
	PCA1	**0.869**	−	**0.004**
Physical defensive traits	PCA2	0.480	−	0.079
	PCA3	0.496	−	0.070
	PCA1	**1.253**	−	**0.001**
All traits	PCA2	**0.796**	−	**0.002**
	PCA3	**0.716**	−	**0.007**
Secondary metabolites	−	−	-0.114	0.910

Notes: Values significantly are indicated in bold ($P < 0.05$).

TABLE S13. Phylogenetic signal of 40 functional traits

Traits	K-value	p-value	Groups	Phylogenetic signals
ADL	0.454	0.119	Physical defence	N
Hemicellulose	1.047	0.001	Physical defence	Y
Cellulose	0.417	0.177	Physical defence	N
Si	0.544	0.038	Physical defence	Y
Thickness	0.419	0.264	Physical defence	N
Toughness	0.439	0.168	Physical defence	N
Upper.epi	0.282	0.631	Physical defence	N
Lower.epi	0.256	0.738	Physical defence	N
C	1.059	0.001	Resource acquisition	Y
N	0.643	0.013	Resource acquisition	Y
C:N	0.529	0.049	Resource acquisition	Y
N:P	0.368	0.323	Resource acquisition	N
P	0.316	0.594	Resource acquisition	N
K	0.854	0.002	Resource acquisition	Y
Ca	0.589	0.023	Resource acquisition	Y
Mg	0.745	0.018	Resource acquisition	Y
SLA	0.255	0.859	Resource acquisition	N
Fresh mass	0.216	0.928	Resource acquisition	N
Dry mass	0.229	0.861	Resource acquisition	N
Leaf area	0.214	0.901	Resource acquisition	N
LDMC	0.488	0.074	Resource acquisition	N
Chlorophyll	0.489	0.082	Photosynthetic	N
PT	0.615	0.04	Photosynthetic	Y
ST	0.683	0.011	Photosynthetic	Y
R	0.475	0.122	Photosynthetic	N
A_{max}	0.382	0.389	Photosynthetic	N
Ls	1.025	0.001	Photosynthetic	Y
CO	1.294	0.001	Photosynthetic	Y
Max height	0.418	0.426	Photosynthetic	N
WUE	1.007	0.002	Hydraulic	Y
Conductance	0.481	0.086	Hydraulic	N
swc	0.731	0.004	Hydraulic	Y
π_o	0.906	0.001	Hydraulic	Y
π_{tlp}	0.990	0.001	Hydraulic	Y
RWC	0.999	0.002	Hydraulic	Y
Elasticity modulus	0.573	0.041	Hydraulic	Y
C_{ft}	0.775	0.004	Hydraulic	Y
C_{tlp}	1.015	0.001	Hydraulic	Y
$C_{ft}*$	0.835	0.008	Hydraulic	Y
Wood density	0.351	0.415	Hydraulic	N
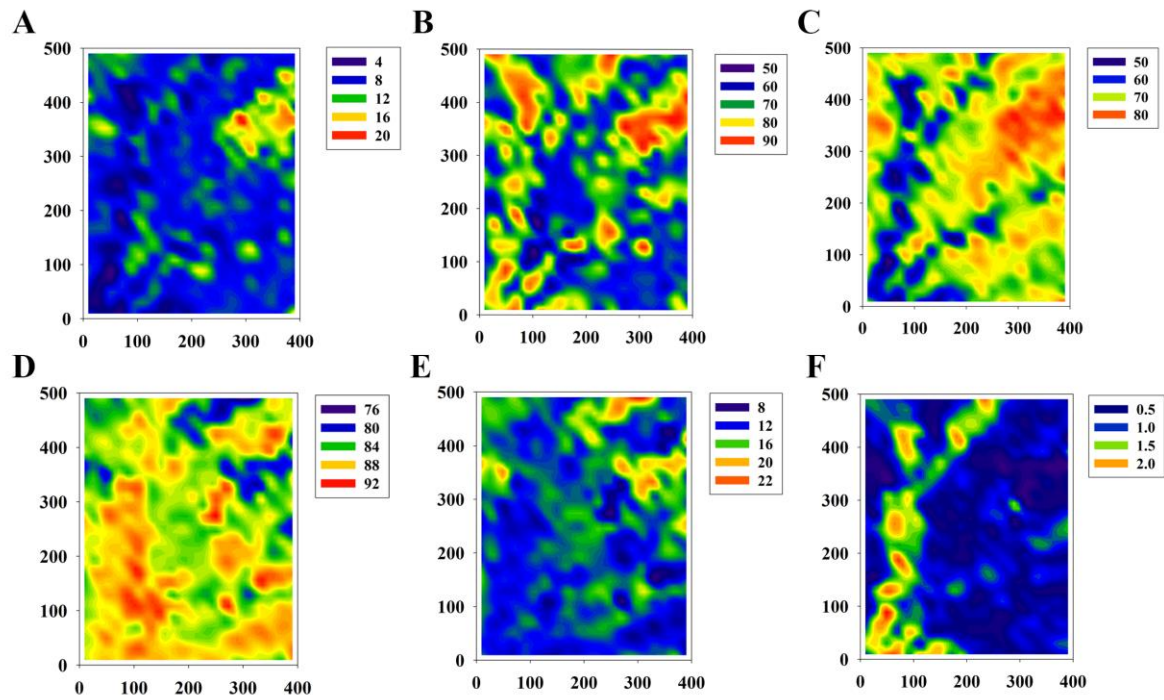
FIGURE S1. Patterns of herbivory pressure. A: average herbivory ratio; B: hole ratio; C: marginal

ratio; D: generalized ratio; E: intermediate ratio; F: specialized ratio.

LITERATURE CITED

Abramoff, M., Magalhães, P. & Ram, S.J. (2004). Image processing with ImageJ. *Biophotonics International*, 11, 36-42.

Alvarez-Yepiz, J.C., Burquez, A. & Dovciak, M. (2014). Ontogenetic shifts in plant-plant interactions in a rare cycad within angiosperm communities. *Oecologia*, 175, 725-735.

Bartlett, M.K., Scoffoni, C., Ardy, R., Zhang, Y., Sun, S., Cao, K. *et al.* (2012a). Rapid determination of comparative drought tolerance traits: using an osmometer to predict turgor loss point. *Methods in Ecology and Evolution*, 3, 880-888.

Bartlett, M.K., Scoffoni, C. & Sack, L. (2012b). The determinants of leaf turgor loss point and prediction of drought tolerance of species and biomes: a global meta-analysis. *Ecology Letters*, 15, 393-405.

Cao, X., Jia, J.B., Li, H., Li, M.C., Luo, J., Liang, Z.S. *et al.* (2012). Photosynthesis, water use efficiency and stable carbon isotope composition are associated with anatomical properties of leaf and xylem in six poplar species. *Plant Biology*, 14, 612-620.

Chave, J. (2005). Measuring wood density for tropical forest trees. *A field manual for the CTFS sites*, 1-7.

Choong, M.F. (1996). What makes a leaf tough and how this affects the pattern of *Castanopsis fissa* leaf consumption by caterpillars. *Functional Ecology.*, 10, 668-674.

Cornelissen, J.H.C., Lavorel, S., Garnier, E., Diaz, S., Buchmann, N., Gurvich, D.E. *et al.* (2003). A handbook of protocols for standardised and easy measurement of plant functional traits worldwide. *Australian Journal of Botany*, 51, 335-380.

Croft, H., Chen, J.M., Luo, X., Bartlett, P., Chen, B. & Staebler, R.M. (2017). Leaf chlorophyll content as a proxy for leaf photosynthetic capacity. *Global Change Biology*, 23, 3513-3524.

Debona, D., Rodrigues, F.A. & Datnoff, L.E. (2017). Silicon's role in abiotic and biotic plant stresses. *Annual Review of Phytopathology*, 55, 85-107.

Drake, J.E., Power, S.A., Duursma, R.A., Medlyn, B.E., Aspinwall, M.J., Choat, B. *et al.* (2017). Stomatal and non-stomatal limitations of photosynthesis for four tree species under drought: A comparison of model formulations. *Agricultural and Forest Meteorology*, 247, 454-466.

James, S.A. & Bell, D.T. (2000). Influence of light availability on leaf structure and growth of two *Eucalyptus globulus* ssp globulus provenances. *Tree Physiology*, 20, 1007-1018.

Kitajima, K., Llorens, A.M., Stefanescu, C., Timchenko, M.V., Lucas, P.W. & Wright, S.J. (2012). How cellulose-based leaf toughness and lamina density contribute to long leaf

lifespans of shade-tolerant species. *New Phytologist*, 195, 640-652.

Kolb, K.J., Sperry, J.S. & Lamont, B.B. (1996). A method for measuring xylem hydraulic conductance and embolism in entire root and shoot systems. *Journal of Experimental Botany*, 47, 1805-1810.

Kula, A.A.R., Hey, M.H., Couture, J.J., Townsend, P.A. & Dalgleish, H.J. (2020). Intraspecific competition reduces plant size and quality and damage severity increases defense responses in the herbaceous perennial, *Asclepias syriaca*. *Plant Ecology*, 221, 421-430.

Lau, R.R. & Young, D.R. (1988). Influence of physiological integration on survivorship and water relations in a clonal herb. *Ecology*, 69, 215-219.

Lawson, J.R., Fryirs, K.A. & Leishman, M.R. (2015). Hydrological conditions explain variation in wood density in riparian plants of south-eastern Australia. *Journal of Ecology*, 103, 945-956.

Li, Y., Song, X., Li, S., Salter, W.T. & Barbour, M.M. (2020). The role of leaf water potential in the temperature response of mesophyll conductance. *New Phytologist*, 225, 1193-1205.

Li, Z.-X., Yang, W.-J., Ahammed, G.J., Shen, C., Yan, P., Li, X. *et al.* (2016). Developmental changes in carbon and nitrogen metabolism affect tea quality in different leaf position. *Plant Physiology and Biochemistry*, 106, 327-335.

Liu, Y., Xiao, J., Ju, W., Zhou, Y., Wang, S. & Wu, X. (2015). Water use efficiency of China's terrestrial ecosystems and responses to drought. *Scientific Reports*, 5, 13799.

Lo Gullo, M. & Salleo, S. (1988). Different strategies of drought resistance in three Mediterranean sclerophyllous trees growing in the same environmental conditions. *New Phytologist*, 108, 267-276.

Lusk, C.H. & Reich, P.B. (2000). Relationships of leaf dark respiration with light environment and tissue nitrogen content in juveniles of 11 cold-temperate tree species. *Oecologia*, 123, 318-329.

Moore, B.D., Andrew, R.L., Külheim, C. & Foley, W.J. (2014). Explaining intraspecific diversity in plant secondary metabolites in an ecological context. *New Phytologist*, 201, 733-750.

Poorter, L., Bongers, F., Sterck, F.J. & WÖLl, H. (2005). Beyond the regeneration phase: differentiation of height–light trajectories among tropical tree species. *Journal of Ecology*, 93, 256-267.

Porra, R.J., Thompson, W.A. & Kriedemann, P.E. (1989). Determination of accurate extinction coefficients and simultaneous-equations for assaying chlorophyll-a and chlorophyll-b

extracted with 4 different solvents - verification of the concentration of chlorophyll standards by atomic-absorption spectroscopy. *Biochimica Et Biophysica Acta*, 975, 384-394.

Reich, P.B. (2014). The world-wide 'fast-slow' plant economics spectrum: a traits manifesto. *Journal of Ecology*, 102, 275-301.

Richards, L.A., Dyer, L.A., Forister, M.L., Smilanich, A.M., Dodson, C.D., Leonard, M.D. *et al.* (2015). Phytochemical diversity drives plant-insect community diversity. *Proceedings of the National Academy of Sciences of the United States of America*, 112, 10973-10978.

Sack, L., Cornwell, W.K., Santiago, L.S., Barbour, M.M., Choat, B., Evans, J.R. *et al.* (2010). A unique web resource for physiology, ecology and the environmental sciences: PrometheusWiki. *Functional Plant Biology*, 37, 687-693.

Sack, L., Pasquet-Kok, J. & Contributors, P. (2011). Leaf pressure-volume curve parameters. *PrometheusWiki website: http://prometheuswiki. org/tiki-index. php*.

Scholander, P.F., Bradstreet, E.D., Hemmingsen, E. & Hammel, H. (1965). Sap Pressure in Vascular Plants: Negative hydrostatic pressure can be measured in plants. *Science*, 148, 339-346.

Sedio, B.E., Boya P, C.A. & Rojas Echeverri, J.C. (2018). A protocol for high-throughput, untargeted forest community metabolomics using mass spectrometry molecular networks. *Applications in Plant Sciences*, 6, e1033.

Sedio, B.E., Echeverri, J.C.R., Boya, C.A.P. & Wright, S.J. (2017). Sources of variation in foliar secondary chemistry in a tropical forest tree community. *Ecology*, 98, 616-623.

Sims, D.A. & Gamon, J.A. (2002). Relationships between leaf pigment content and spectral reflectance across a wide range of species, leaf structures and developmental stages. *Remote Sensing of Environment*, 81, 337-354.

Smith, N.G. & Dukes, J.S. (2013). Plant respiration and photosynthesis in global-scale models: incorporating acclimation to temperature and CO2. *Global Change Biology*, 19, 45-63.

Speed, M.P., Fenton, A., Jones, M.G., Ruxton, G.D. & Brockhurst, M.A. (2015). Coevolution can explain defensive secondary metabolite diversity in plants. *New Phytologist*, 208, 1251-1263.

Vrede, T., Dobberfuhl, D.R., Kooijman, S.A.L.M. & Elser, J.J. (2004). Fundamental connections among organism C:N:P stoichiometry, macromolecular composition, and growth. *Ecology*, 85, 1217-1229.

Wang, M., Carver, J.J., Phelan, V.V., Sanchez, L.M., Garg, N., Peng, Y. *et al.* (2016). Sharing

and community curation of mass spectrometry data with Global Natural Products Social Molecular Networking. *Nature Biotechnology*, 34, 828-837.

Wright, I.J., Reich, P.B., Westoby, M., Ackerly, D.D., Baruch, Z., Bongers, F. *et al.* (2004). The worldwide leaf economics spectrum. *Nature*, 428, 821-827.